THE UNIVERSITY OF ADELAIDE

GEOLOGICAL SETTING OF THE LATE PROTEROZOIC WONOKA FORMATION AT PICHI RICHI PASS, SOUTHERN FLINDERS RANGES, SOUTH AUSTRALIA: GEOCHEMICAL, STABLE ISOTOPE AND DIAGENETIC ANALYSIS

by D. AYLIFFE, B.Sc.

November, 1992

D. M. McKirdy

Geological setting of the late Proterozoic Wonoka Formation carbonate ramp and canyon sequence at Pichi Richi Pass Southern Flinders Ranges, South Australia: geochemical, stable isotope, and diagenetic analysis.

Damien Ayliffe B. Sc.

This thesis is submitted as partial
fulfilment of requirements for the Honours Degree
of Bachelor of Science

Department of Geology and Geophysics,
University Of Adelaide
13th November 1992

National Grid Reference:
Port Augusta sheet S1 53-4 (1 : 250 000)
Orroroo sheet S1 54-1 (1 : 250 000)

List of Figures

List of Figures cont.

List of Tables

List of Plates

List of Enclosures

Abstract

Carbon, oxygen and strontium isotope stratigraphy has increased the resolution of Proterozoic stratigraphic correlation. Isotopic analysis was performed on the late Proterozoic Wonoka Formation canyon and carbonate platform sequences .Highly depleted and homogenised carbon and oxygen isotopes characterise the canyon fill ($\delta^{13}C$ = -8 to -7‰ $\delta^{18}O$ = - 17 to -15‰ PDB) whilst a major positive excursion was observed in the Wonoka Formation carbonate platform sequence ($\delta^{13}C$= -8 to -0.5‰, $\delta^{18}O$ = -15.0 to -7.0‰ PDB). These values correlate closely with other established isotopic trends throughout the Adelaide Geosyncline. However similar aged late Vendian strata throughout the world show low positive values.

Strontium isotopic analysis revealed relatively ^{87}Sr enrichment in the carbonate platform deposits compared to the canyon sequence .This was attributed to the input of ^{87}Sr enriched terrestrially derived strontium. The ^{87}Sr / ^{86}Sr ratio of the Wonoka Formation correlates closely with established late Proterozoic seawater trends. Therefore a primary strontium isotopic composition is implied for the Wonoka Formation

Major and trace element geochemical analysis (Ca, Mg, Sr, Fe, Mn, and Rb) was performed to assess the diagenetic alteration of the late Proterozoic strata. Samples with low Mn/Sr,high Ca/Sr, high strontium, and low rubidium have the highest probability of preserving a primary geochemical signal. Most samples from the Pichi Richi region analysed plotted under the altered Mn/Sr (<2) and Ca/Sr (<2000) values.

The high remnant strontium concentrations of the Wonoka Formation suggest neomorphism from an aragonitic precursor. Micritic carbonate of the Wonoka Formation was probably a primary marine precipitate of aragonite derived from late Proterozoic supersaturated seas. Therefore the majority of sediment diagenesis probably occurred in the marine phreatic zone, resulting in the observed primary isotopic composition.

Contents

Contents

Chapter 1 Introduction

Until recently recognition of equivalent late Proterozoic sedimentary sequences was based on broad scale lithostratigraphic correlations. Our poor understanding of Proterozoic stratigraphy is primarily due to the paucity of biostratigraphic control before the Cambrian. Proterozoic stratigraphy has therefore traditionally relied upon lithostratigraphy, sequence stratigraphy, geochronological dating of igneous rock and tuff layers and a limited biostratigraphy of stromatolites, acritarch microfossils and the soft-bodied Ediacaran fauna (Knoll and Walter, 1992).

Recently, however, secular variation of geochemical signals encoded in carbonates, particularly their stable carbon and oxygen isotope ratios, have been used in the correlation of Proterozoic sediments. The isotopic composition of unaltered marine carbonates reflects the isotopic composition of the seawater from which they precipitated. Therefore the variation in the primary carbon and oxygen isotope signatures of such carbonates through the geological record enables both intra and inter-basinal correlation.

Carbon and oxygen isotope stratigraphies of many of the major geological boundaries of the Phanerozoic have been published, notably the Cretaceous / Tertiary, Permian/Triassic and Ordovician/Devonian transitions (Magaritz, 1989, 1990) Magaritz et al. (1992). The Precambrian / Cambrian boundary, on the other hand, had been relatively neglected due to the likelihood of diagenetic overprinting. Numerous isotope stratigraphies of this transition have now been documented by Aharon et al. (1986), Lambert et al. (1987), Magaritz et al. (1986,1988), Knoll et al. (1986), Brasier et al. (1990, 1992), Fairchild et al. (1990), Knoll (1991) Kaufman et al. (1992) and Brasier (1992) enabling high resolution stratigraphic correlation of this most important period in earth history.

Another useful geochemical tool in stratigraphic correlation is the $^{87}Sr / ^{86}Sr$ ratio. Knoll (1991), Derry et al. (1989), Derry et al. (1992), Kaufman et al. (1992) and Asmerom et al. (1991), have all used the secular variation in strontium isotopes in Proterozoic strata to correlate sequences from widespread localities. Variation in strontium in the Phanerozoic has been quite conservative compared to that of the Proterozoic.

Depositional environment and post-depositional diagenesis may greatly effect the isotopic composition of carbonates. Several phases of cementation in different diagenetic environments may give rise to a completely different isotopic signal. Late-stage burial and metamorphism at elevated temperatures may also drastically alter the original isotopic composition. Therefore, in any reputable geochemical study, the effect of post-depositional cementation and other diagenetic processes on the primary geochemical signal must be established.

This study concentrates on the late Proterozoic Wonoka Formation of the Adelaide Geosyncline, Wilpena Group. The main study area is in the Saltia, Pichi Richi Pass and Richman Valley areas of the Southern Flinders Ranges, South Australia (Fig. 1). Several geological sections were measured and a geological map of the Proterozoic Wonoka Formation canyon and carbonate ramp sequences was prepared. Sampling along sections of relatively homogeneous limestone was carried out for geochemical and isotopic analysis.

This study encompassed several geochemical techniques including stable carbon, oxygen and strontium isotopic analyses. Stratigraphic profiles of the oxygen and carbon isotopic ratios were constructed to enable chemostratigraphic correlation of the late Proterozoic Wonoka Formation. Carbonate mineralogy was determined using X-ray diffraction and percentage carbonate by loss on ignition. The effect of diagenesis on the primary isotopic signals was established by using major and trace element analyses. Petrographic and cathodoluminescence techniques were also used to assess the preservation of samples selected for the above analyses.

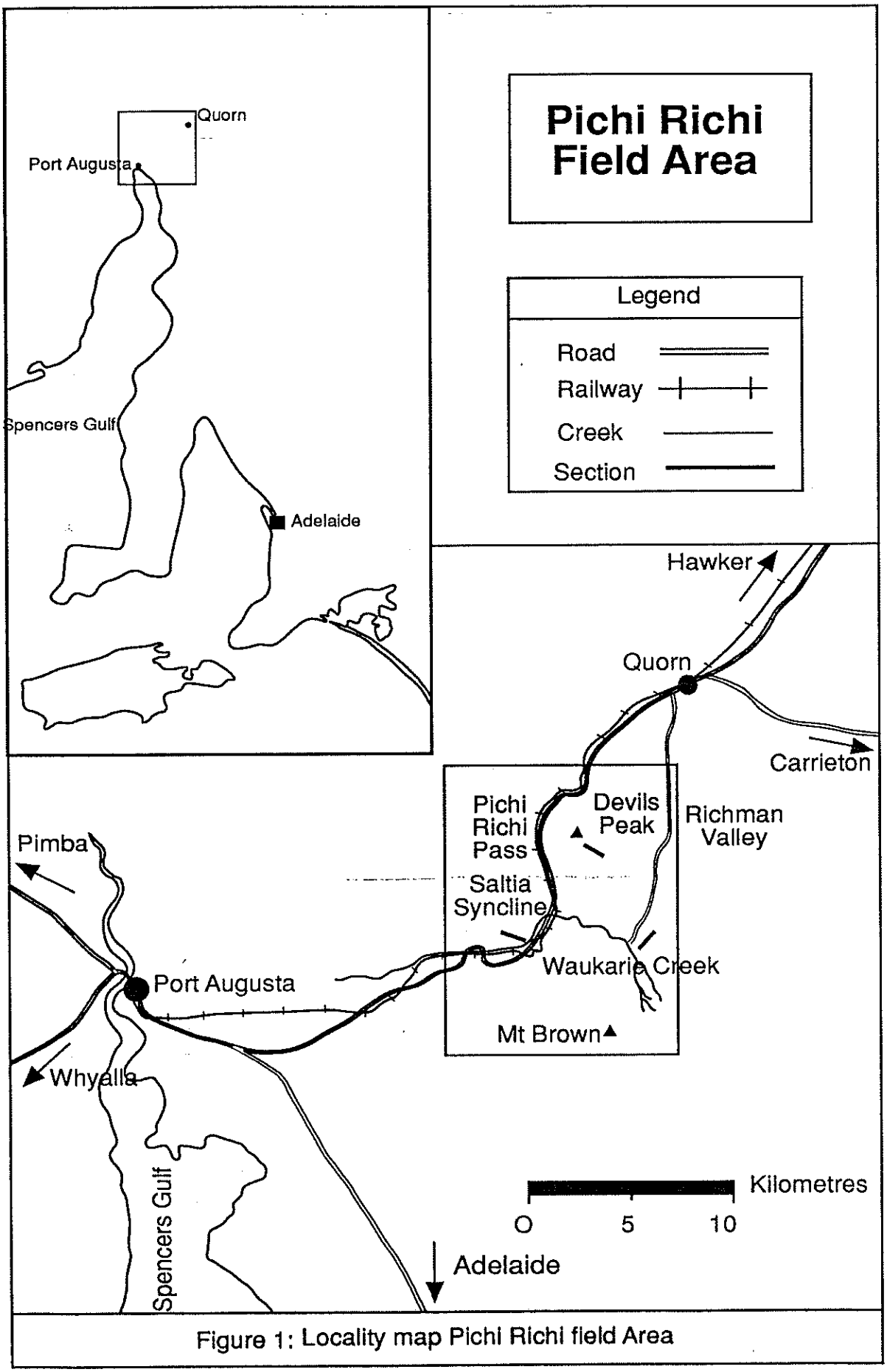

Figure 1: Locality map Pichi Richi field Area

Chapter 2: Geological Setting and Previous Investigations

The late Proterozoic / Cambrian transition is a time of immense global geologic, atmospheric, and biological change. The upper Proterozoic is globally characterised by low-latitude supercontinents, widespread glaciation , and associated low stands of sealevel (Brasier, 1992). Gradual warming of the atmosphere and the first appearance of abundant fossils including the soft bodied Ediacaran Fauna, occurred in the latest Precambrian (Tucker, 1992). In contrast, the Cambrian is characterised by the first appearance of skeletal fossils, abundant trace fossils, a high stand of sea level, a global greenhouse climate, the break up of supercontinents and the opening of oceans (Brasier, 1992).

The Adelaide Geosyncline is of late Proterozoic to Middle Cambrian age. The sediments of the Adelaide Geosyncline have been interpreted by various authors as being deposited in a rift or failed rift tectonic setting (von der Borch et al., 1982; Preiss 1987; and von der Borch et al. 1988). One mechanism for the formation of the Adelaide Geosyncline recently proposed by Jenkins (1990) involved periods of lithostatic extension and thermal subsidence. These Proterozoic and Cambrian sediments were subsequently folded and deformed during the Cambro-Ordovician Delamerian Orogeny approximately 515-490 Ma ago (Preiss, 1987; Jenkins, 1990). Renewed uplift during late Cenozoic time formed the north / south trending belt of thick late Proterozoic to Cambrian sediments now exposed in the Flinders Ranges and Adelaide Hills.

The Umberatana and Wilpena Groups as defined by Dalgarno and Johnson (in Thompson, 1964) form the uppermost Proterozoic sequences of the Adelaide Geosyncline, the Heysen Supergroup of Preiss. The upper Umberatana Group contains the Marinoan glacials of the Elatina Formation. These glacial sediments may be correlated with other glacial strata of world wide extent, collectively known as the Varangian. The Umberatana Group is conformably overlain by the latest Proterozoic Wilpena Group which forms the Ediacarian of Cloud and Glaessner (1982).

The Wilpena Group comprises sediment deposited during two major transgressive and regressive cycles. The lower cycle comprises the Nuccaleena Formation, Brachina Formation, and ABC Range Quartzite together which form the Brachina Subgroup (Plummer, 1978). The upper transgressive / regressive cycle comprises the Bunyeroo Formation, Wonoka Formation and the Pound Subgroup of Jenkins and Gostin (1983). Jenkins (1981) erected the Ediacaran Period which corresponds to the Wonoka Formation and Pound Subgroup units, the Bonney Sandstone and Rawnsely Quartzite. The Pound Subgroup is the youngest Precambrian sequence of the Adelaide Geosyncline.

This study concentrates on the second regressive sequence of the Wilpena Group, the Wonoka Formation. This is a mixed carbonate - siliciclastic sequence which in the central and southern Flinders Ranges was deposited on a carbonate shelf or platform (Preiss, 1987). Haines (1986, 1987, 1988) interpreted the Wonoka Formation as being deposited on a storm-dominated shelf showing cycles of storm and event bed deposition. In the present study, eleven mappable lithostratigraphic units recognised by Haines (1986, 1987) have been adopted to describe the shelf sequence.

Coats (cited in Thompson, 1964) first described a large-scale slump structure in the Wonoka Formation from the Patsy Springs region east of Copley, which he later recognised as a submarine canyon Coats (1973). Numerous canyons have subsequently been identified and mapped throughout much of the Flinders Ranges and the adjacent Officer Basin by various workers including von der Borch et al. (1982), Gostin and Jenkins (1983), von der Borch and Grady (1984), von der Borch et al. (1985, 1989), Haines (1986, 1987, 1990), Eickoff et al. (1988), DiBona (1990) Christie-Blick et al. (1990) and Sukanta et al. (1991).

Several canyon incision models have been proposed by Coats (1973), von der Borch and Grady (1984), von der Borch et al. (1982, 1985, 1989), Gostin and Jenkins (1983), Eickoff et al. (1988), Christie-Blick et al. (1990), and Di Bona (1990). There are two major schools of thought on the origin of the canyon structures; submarine and subaerial. Schematic representations of the two different modes of canyon formation are shown in Figure 2 (after von der Borch et al., 1982, and Christie-Blick et al., 1990) and discussed below.

Figure 2: Proposed models for the formation of late Proterozoic Wonoka formation canyons

1) Submarine incision after von der Borch et al. (1982)

A) Progradation of Brachina Formation.

B) Fall in sea level in early Wonoka time and intial canyon incision by proximal turbidites.

C) Sea level rise progradation of slope and increased canyon erosion.

D) Coastal onlap and backfilling of canyons by submarine fan sequences.

2) Subaerial canyon incision model after Christie-Blick et al. (1990).

A) Deep basin and ramp of early Wonoka time immediately before canyon incision.

B) A large fall in sea level due to evaporitic drawdown exposes the early Wonoka Formation and underlying strata to erosion and canyon incision.

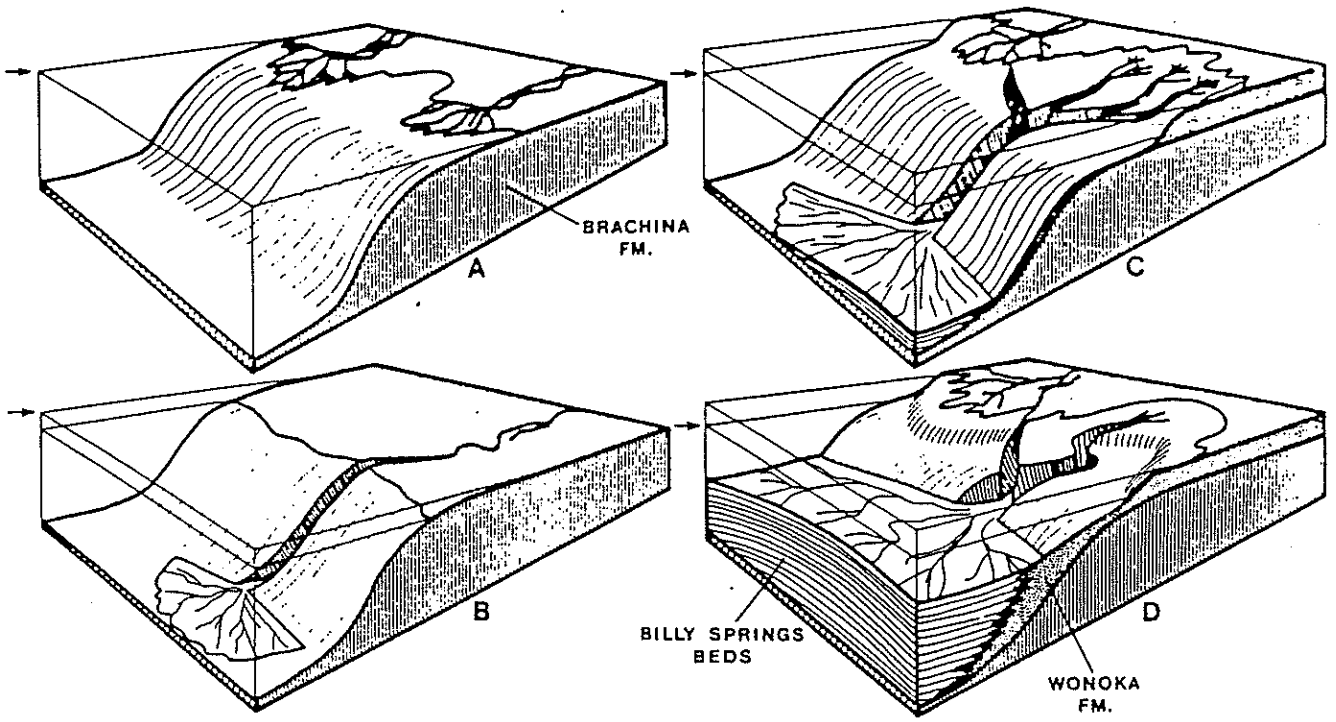

A. IMMEDIATELY BEFORE CANYON-CUTTING EVENT

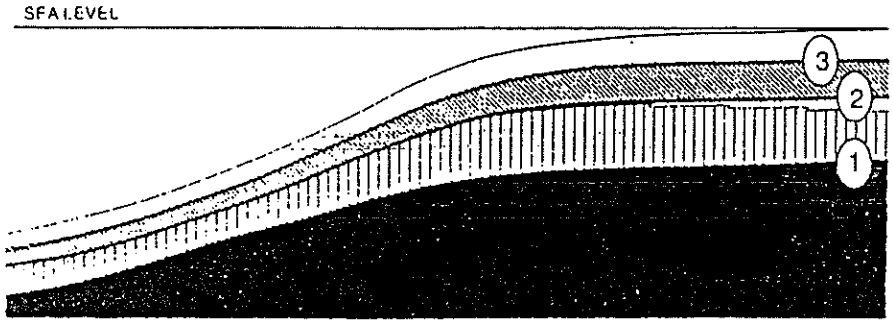

B. DURING CANYON-CUTTING EVENT

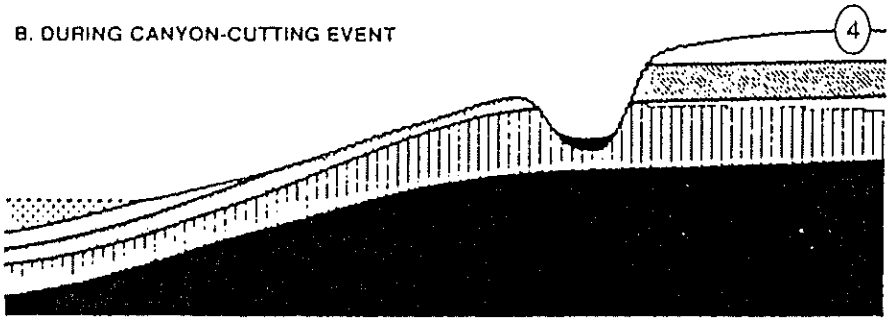

LOWSTAND EVAPORITES

NON MARINE SEDIMENT AT BASE OF FLUVIALLY INCISED CANYON

WONOKA FORMATION (UNITS 2 AND 3)

BUNYEROO FORMATION (PLUS UPPERMOST ABC RANGE QUARTZITE AND WONOKA UNIT 1)

ABC RANGE QUARTZITE

NUCCALEENA AND BRACHINA FORMATIONS, ULDIA SILTSTONE

UMBERATANA GROUP

SEQUENCE BOUNDARY OR EROSION SURFACE

illegible

Coats (1973), von der Borch et al. (1982), Preiss (1987) and Haines (1987) all attributed the canyon formation to submarine processes. This model was based upon apparent similarities between the Wonoka Canyons and modern analogues observed in the Bahamas and Indonesia. The presence of thick bedded sandstones, interpreted as deep water turbidites, in the canyon-fill sediments also support this model. Eickoff et al (1988) and von der Borch et al (1985, 1989), however, questioned this submarine model and instead proposed a model for canyon formation involving subaerial incision.

A submarine model of canyon formation was elaborated by von der Borch et al. (1982). In this model, a significant drop in sea level during early Wonoka time caused sediment load to be deposited straight onto the ramp slope. Submarine turbidity currents caused down cutting and lateral erosion of the underlying strata and hence canyon formation. Classic Bouma sequences and the association of sandstones and shale in the basal canyon fill were cited as evidence for a submarine origin of the Wonoka canyons.

The presence of meandering channels, axial conglomerates of possible fluviatile origin (von der Borch, 1985), alternation of flute cast and palaeocurrent directions by approximately 180°, oscillation ripples and hummocky cross stratification in the basal canyon fill, casts doubt on the submarine origin of these canyons. Eickoff et al. (1988) noted a carbonate wallplaster or layer coating the canyon wall which had extremely negative carbon and oxygen isotopes values ($\delta^{13}C$ = -8.86‰, $\delta^{18}O$ = -15.43‰) which could not be of marine origin. DiBona (1990) observed the Burr Well member and reported tepee structures and stromatolites of supposedly peritidal origin. Eickoff et al. (1988) and DiBona (1990) cited the above discrepancies, especially the alternating flute cast directions and meandering nature, as evidence supporting a subaerial incision for the Wonoka canyons.

According to Eickoff et al. (1988) a fall in sea level of approximately 1 kilometre during early to middle Wonoka time is required for subaerial erosion. During this low stand in sea level, river channels meandered across the newly exposed platform and cut through the underlying strata. Subaerial exposure of the canyon walls allowed precipitation of a calcrete layer (the wallplaster) which now coats the canyon walls. Deposition by mass flow and fluvial processes would account for the observed structures and meandering nature of many of the unique structures

mentioned above. Subsequent sea level rise during middle Wonoka time then filled the canyons by coastal onlap.

A major problem with the hypothesis of subaerial canyon formation is that global eustacy cannot explain fluctuations in sea level of the required magnitude. Another problem with subaerial incision is that there is no evidence for such large scale fluctuations in sea level during early Wonoka time. Von der Borch et al. (1989) and Christie Blick et al. (1990) suggested that the large fall in sea level could be explained by an evaporitic draw down similar to that of the Messinian event which drained the Mediterranean. Christie Blick (1990) and von der Borch (pers. comm.) have proposed numerous lower order sequence boundaries through the Wonoka canyon fill associated with fluviatile sandstone lenses in the Patsy Spring canyon.

Haines (1987) is one of the most recent authors to explain the Wonoka canyons in terms of a submarine origin. Sedimentary textures used to support a subaerial origin, in particular alternating current directions and meandering channels, have been observed in the modern marine environment . The lack of karst topography in the supposedly subaerially exposed lower Wonoka is another factor which casts doubt upon the subaerial model of canyon formation (R.J.F. Jenkins pers. comm.). Jansyn (1990) mapped thickness variations in the Wilpena Trough in the central Flinders Ranges and suggested that canyon formation may be fault related.

Chapter 3: Stratigraphy of the Wilpena Group

The Pichi Richi Pass study area is composed of late Proterozoic sediments belonging to the Umberatana and Wilpena Groups. The stratigraphy of the Wilpena Group near Pichi Richi Pass and Bunyeroo Gorge is shown in Figure 3 and briefly described below.

3.1 Nuccaleena Formation

The Nuccaleena Formation is the basal unit of the Wilpena Group. It conformably overlies the Marinoan glacial diamictite and tillites of the Elatina Formation and indicates a warming of the latest Proterozoic climate (Preiss, 1987). This thin (10 cm - 10 m) but persistent dolostone represents several depositional environments ranging from supratidal to subtidal.

3.2 Brachina Formation

The Brachina Formation is a finely laminated, red or green shale with minor calcareous intervals which crop out in the centre of a large anticline in Pichi Richi Pass (see map). It has a pencil-like appearance due to the intersection of bedding and cleavage which formed during the Delamerian Orogeny . It is interpreted as a basinal deposit of a transgresssive systems tract (Preiss, 1987). In the northern Flinders Ranges, the Brachina Formation and the immediately overlying units have been significantly eroded and incised by the so-called Wonoka canyons (von der Borch et al., 1982).

3.3 ABC Range Quartzite

In the Pichi Richi Pass area, the ABC Quartzite is a white to pale orange feldspathic quartzite with heavy mineral banding and micaceous lamination . Numerous sedimentary structures including planar, trough, and herring bone cross bedding, mud cracks and truncated lensoidal sandstone beds suggest a shallow tidal flat to fluviatile environment. Intensely brecciated and altered along fault zones with slickenslides, vein growth fibres perpendicular to principal compressive stress direction and specular haematite veins, the ABC Quarzite has been strongly deformed and uplifted and now forms many of the high ridges in the Flinders Ranges. In the study area, the ABC Range Quartzite is commonly unconformably overlain by Wonoka Formation due to erosion associated with canyon incision (Plate 2.6).

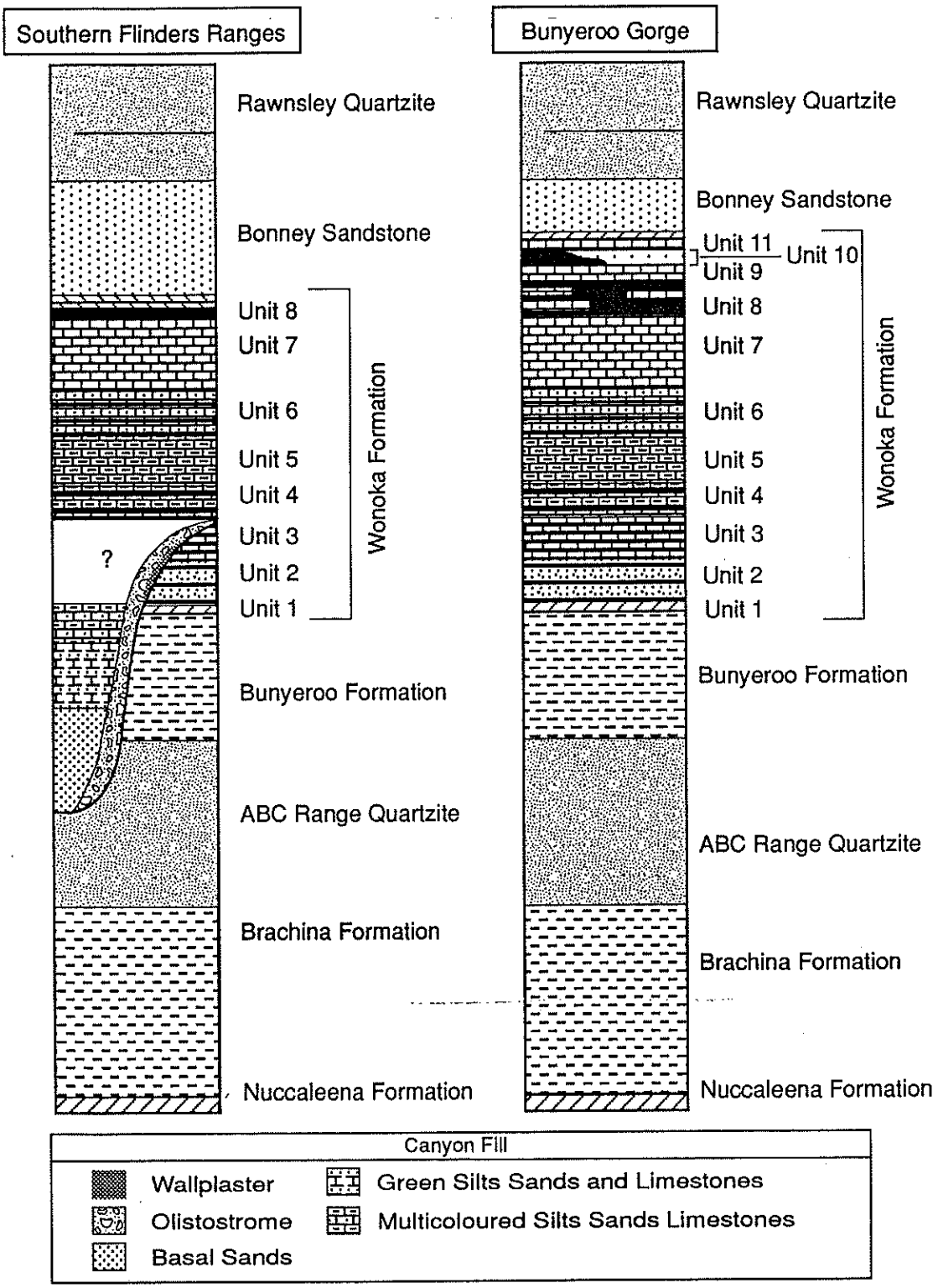

Figure 3: Stratigraphy of the Wilpena Group Southern Flinders Ranges and Bunyeroo Gorge (after Haines, 1986).

3.4 Bunyeroo Formation

The finely laminated silts of the Bunyeroo Formation are rarely exposed in the Pichi Richi area due to canyon cutting and local faulting. Waukarie Creek is the only locality in the field area where the Bunyeroo Formation was observed. At Waukarie Creek, the Bunyeroo Formation conformably overlies the ABC Range Quartzite and is itself overlain by Wonoka Formation. The stratigraphy is not complete as canyon cutting has deeply eroded and incised the early Wonoka Formation, the Bunyeroo Formation and the underlying ABC Range Quartzite.

At Waukarie Creek the Bunyeroo Formation also contains a thin 'tuffaceous' layer approximately 80 m from its base. This layer contains abundant clasts of Gawler Range Volcanics and shocked quartz and has been interpreted as the ejecta from the Lake Acraman impact (Gostin et al., 1986 ; Williams, 1986). The Acraman ejecta layer has been detected in core from the Officer Basin and provides a unique stratigraphic marker for correlation with the Adelaide Geosyncline (Wallace et al., 1989).

3.5 Wonoka Formation

The Wonoka Formation platform sequence in the southern Flinders Ranges includes Haines' units 1-8. The upper parts of the formation (units 9-11) are found only in the Bunyeroo Gorge type section and at localities further to the north (Haines, 1986). Locally the Lower Wonoka, (units 1 to lower unit 3) has been removed by canyon erosion. In the Pichi Richi field area, the Wonoka Formation comprises two main sequences: the canyon facies and carbonate ramp facies.

3.5.1 Canyon Sequence

The canyon facies seem to be unique with no real correspondence to Haines (1987) carbonate shelf units, although he noted a resemblance between mineralogy of the lower canyon sequence and Unit 2. Numerous units have been described in the Wonoka Formation canyons by previous authors, including von der Borch et al. (1982) , von der Borch et al. (1985, 1989), Eickoff et al. (1988), Haines (1986, 1987) and DiBona (1990). In the present study area, many of the canyon sequences are poorly exposed or only the lower portion remains due to faulting and erosion. As a result, canyon units distinctive to this area have been erected but close similarities to those of von der Borch et al. (1982), Haines (1987) and Eickoff et al. (1988) are noted .

Unit A Wallplaster

The wallplaster is restricted to a small outcrop at Waukarie Creek overlying the Bunyeroo / Wonoka Formation canyon cut unconformity. The wallplaster is a massive, white, very fine grained, calcareous layer coating the canyon wall. It contains very little clastic material and has a very high carbonate content of approximately 80%. Eickoff et al. (1988) believe the wallplaster is remnant calcrete which adhered to the canyon wall during subaerial exposure.

Unit B Olistostrome

The olistostrome unit consists of thick, massively bedded, lenticular boulder conglomerates of mixed provenance. Clasts up to 3 metres in size of presumed early Wonoka Formation, Bunyeroo, and ABC Range Quartzite were derived by the erosion of the underlying strata during canyon incision (Plate1.1-1.2). As reported by von der Borch et al. (1982) this unit makes up the basal and canyon wall fill. Unit B was best observed at the base and along many of the walls of canyon incisions, in particular just north of the Pichi Richi South canyon section (see map) and in the Waukarie Creek section. Most of the olistostrome units were interbedded with fine, medium or coarse sandstone of the overlying Unit C.

Unit C - Basal Sands

Overlying many of the canyon cut unconformities are thickly bedded, medium to fine grained calcareous sandstones (Plate 1.3-1.4). Many of the sandstone beds have sharp bases in contact with thin shale units which may be eroded or have water escape structures. Sedimentary structures including parallel and cross laminations, asymmetric climbing ripples (Plate1.4), flute casts (Plate 2.1) and unusual reverse flute casts on bedding surface,or setulfs (Friedman and Sanders 1974) (Plate 2.2) indicate current directions in the canyon fill (plate 2.7-2.8). Ball and pillow structures and slump structures were also observed in outcrop near the Pichi Richi South section (Plate 1.3). These massively bedded sands have been interpreted as possible turbidites (Plate 1.6).

Interbedded with the basal sands and many of the overlying units are grey / green micritic, lenticular, clast-supported intraformational conglomerates with a minor micritic carbonate matrix (Plate 1.5). The intraformational conglomerates did not have any have any distinctive preferred clast orientation other than a compaction fabric. The conglomerates are interpreted as slump or debris flows derived up slope from the carbonate ramp. The tabular nature and rather square ends of the

clasts suggest that they have not been significantly reworked by waves unlike the upper ramp conglomerates.

Unit D - Green silts, fine sands and limestones

The middle of the Pichi Richi South section is characterised by greenish fine silts, sands and limestones (Plate 2.4). Interbedded with the fine sands and limestones are chlorite and muscovite-rich, shale layers, laminated on the centimetre to millimeter scale. A distinctive rhythmical nature was noted for this unit. The fine silts and sands were found to be more calcareous than the finer grained, more micaceous shale layers. Carbonate is dominantly micrite, with equant ferroan calcite cement which has been recrystallized into microspar and sparry calcite. Tabular and lenticular intraformational conglomerates (possibly originally matrix-supported but now dominantly clast-supported), with associated medium sands, were also observed in this unit.

Unit E - Multicoloured Fine Sands Silts and Limestones

A multicoloured grey, green, pink and minor brown unit is the highest canyon fill unit observed in the field area (Plate 2.3). The mainly thin bedded limestones and fine grained sandstones have a reasonably high carbonate content (approximately 40-65 %). This unit crops out mainly in the Saltia Syncline and south of Waukarie Creek immediately west of the Babies Bottom Fault. This poorly exposed unit occurs at the top of the Pichi Richi South and (probably) the Richman Valley sections.

3.5.2 Carbonate Platform Sequence

The carbonate platform sequence in the Pichi Richi field area outcrops to the south and east of Devils Peak (Plate 2.5). This sequence corresponds to units 5-8 of Haines (1987) lithostratigraphic subdivision of the Wonoka Formation and where possible will be referred to in this context.

Unit Transitional

To the south and southeast of Devils Peak is a structurally complex zone of poorly exposed, light coloured Wonoka Formation (Plate 2.5). It is highly cleaved and folded and abundant calcite veins characterise much of the outcrop in this area. Correlation with surrounding areas is difficult. Very limited outcrop is composed of multicoloured, fine grained and thinly bedded calcareous sandstones and limestones.

Unit Transitional cont.

This unit is tentatively interpreted as a transitional unit between canyon fill and the platform sequence. Haines (1987) described a somewhat similar unit from other canyons in the southern Flinders Ranges. Similarities in colour, the nature of the outcrop and sedimentary structures suggests a possible correlation with the multicoloured unit described from the canyons sequence further to the south near Waukarie Creek and in the Saltia syncline (Plate 2.5).

Unit 5 equivalent

This is the lowest recognisable unit of the carbonate platform exposed in the Pichi Richi area, due to faulting in the east and very poor outcrop to the south of Devils Peak. This unit typically consists of fine to medium grained sandstones and limestones with very little interbedded shale. The distinctive reddish coloured sandstones and limestone at the base of the Devils Peak sequence are typical of Haines (1988) unit 5 from other regions in the central and southern Flinders Ranges. Haines (1987) described this unit as displaying cycles of event bed deposition and, in particular, hummocky cross stratification (Plate 2.7-2.8). Minor intraformational conglomerates and stylonodular bedding were also observed.

Unit 6 equivalent

This unit comprises interbedded sandstone and shale that weather brown in outcrop and are usually covered with orange or green lichen indicative of their increased quartz content. On fresh surfaces of the calcite-cemented sandstones fine quartz grains and black flecks (probably mica) are visible. This unit is characterised by a high proportion of shales in the Devils Peak section, enabling it to be distinguished easily from the surrounding units. Sedimentary structures are sparse but event beds stand out prominently over the interbedded shale. Hummocky cross stratification is less common than in the overlying and underlying units.

Unit 7 equivalent

A sequence of mainly grey / green limestones with slightly coarser red limestones is equivalent to Haines (1987) unit 7. Numerous sedimentary structures, including extremely abundant intraformational conglomerates, stylonodular bedding and slump structures which increase up section, characterise this unit and make it one of the most distinctive in the Wonoka Formation. Haines (1988) reported that up to 80% of these limestones are effected by stylonodular bedding.

Intraformational conglomerates and stylonodular bedding are probably the result of wave reworking of semi-lithified to lithified hardgrounds (Tucker and Wright, 1990; Tucker 1992). Haines (1988) attributed the formation of stylonodular bedding in unit 7 to this cause. The lenticular micritic carbonate clasts differ from the clasts of the canyon sequence in that they are usually more rounded in shape. This also implies that the limestones of unit 7 show a rapid shallowing, from the deeper water, event bed deposition to shallower water facies where wave reworking occurred.

Unit 8 equivalent

A higher carbonate content and a corresponding decrease in siliciclastic material characterise this unit, probably as a result of progradation of the shallow water carbonate factory. The presence of cryptalgal laminites, ooids and algal mud flakes towards the top of the unit (N.M.Lemon, pers. comm.) also supports this hypothesis. This unit is capped by khaki / yellow shales and a yellowish/ brown weathering dolomite which are interpreted as being deposited in a fresh-seawater mixing zone or supratidal environment. Rounded intraformational conglomerate was observed near the top of the unit is possibly the result of a wave reworkng of tidal mud flat.

3.6 Bonney Sandstone

Abruptly overlying the calcareous Wonoka Formation is the red terrigenous Bonney Sandstone. This, and the overlying Rawnsley Quartzite, are prograding shoreline sediments deposited during the latest Proterozoic marine regression. The shaley basal sediments of the Bonney Sandstone probably represent a shallow mudflat environment (Haines 1987).

3.7 Rawnsely Quartzite

The Rawnsely Quartzite is a clean, white mature quartzite. It represents a marginal marine to terrestrial facies showing silt and mud layers and thicker more quartz-rich beds. Large-scale cross beds characterise the quartz-rich beds. The Rawnsely Quartzite is one of the most important late Proterozoic sediments as it contains fossils of the soft-bodied Ediacara fauna.

Plate 1.

Canyon Units form Pichi Richi field area.

Plate 1.1:

Large Bunyeroo clast (approxmately 3 metres across) from the Waukarie Creek Canyon Olistostrome Unit (hat approximately 50 cm).

Plate 1.2

Tabular micritic intraformational conglomerate clasts from Waukarie Creek Canyon (pen approximately 14 cm).

Plate 1.3

Ball and pillow from Basal Sand Unit of the Wonoka Formation canyon sequence from Pichi Richi South (lens cap 7 cm).

Plate 1.4

Turbidite beds from the Pichi Richi South lower canyon sequence. Note the planar high flow regime (B) overlain by cross bedded and ripple marks of Bouma c beds which are in turn overlain by massively bedded unit A sandstone (hammer 40 cm).

Plate 1.5

Intraformational conglomerate overlain by massively bedded fine grained calcareous sandstone of the Pichi Richi South Canyon sequence (hammer 40cm).

Plate 1.6

ABC turbidites of the lower canyon sequence Richmond Valley Canyon (lens cap 7 cm).

1.1

1.2

1.3

1.4

1.5

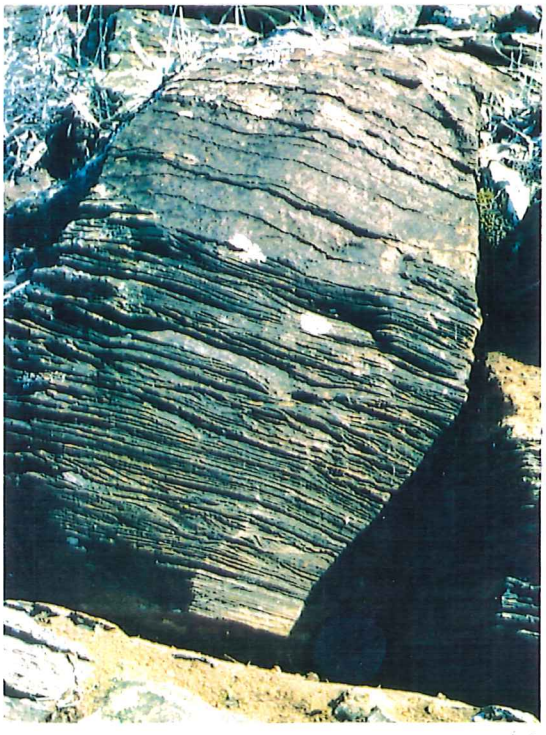

1.6

Plate 2

Plate 2.1:

Flute marks on the base of a calcareous sandstone turbidite bed. Note parallel laminations pass up into ripple cross laminated and parallel sands. Current direction out of page to the top right (hammer 40 cm).

Plate2.2:

Current aligned reverse flute marks or setulfs on the bedding surface of the basal sandstone unit Pichi Richi South canyon. Current direction down page (lens cap 7 cm).

Plate 2.3:

Thinly bedded and finely laminated of fine silt and sandstone unit of the canyon fill (Pichi Richi South Canyon). Note cleavage dips more steeply than bedding (lens cap 7 cm)

Plate 2.4:

Poorly outcropping fine silts and sands of the multicoloured unit upper Wonoka Formation canyon fill, Aulbury Station Saltia Syncline (approximate field of view 1m).

Plate 2.5:

View south over Waukarie Creek and Mt Brown from Devils Peak area. Foreground the cyclic lower carbonate platform, centre the poorly out cropping transitional unit, and background the light hills of the multicoloured upper canyon fill (approximately 6km to Mt Brown).

Plate 2.6:

Light coloured ABC Range Quartzite (bottom of picture) unconformably overlain by the dark Wonoka Formation canyon fill. Canyon cut unconformity is approximately at level of the hammer (hammer 40 cm).

Plate 2.7:

Hummocky cross stratification of lower carbonate platform unit 5. Note the abundance of green lichen indicating the relatively high quartz content (lens cap 7cm).

Plate 2.8:

Hummocky cross stratification of the carbonate platform. Note the low angel truncations (lens cap 7cm).

2.1

2.2

2.3

2.4

2.5

2.6

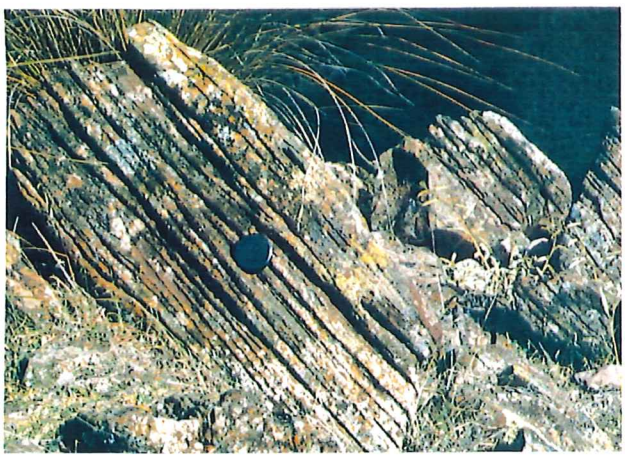

2.7

2.8

Chapter 4: Geochemical Analysis

4.1 Introduction

Three sections were measured through the Pichi Richi South, Richman Valley canyon and Devils Peak platform sequences. Spot sampling using aerial photographs of the Waukarie Creek canyon complex was also performed. Sampling along sections was fairly intense at approximately one sample per 10 metres. Samples selected for analysis were the most carbonate rich, homogeneous and least weathered and altered (i.e. away from calcite veins). The results of samples selected for carbon and oxygen isotopic analysis are shown in Appendix 2 .

4.2 Carbonate Carbon and Total Organic Carbon Analysis

Carbonate isotopic analyses were performed on samples which contained greater than 10% carbonate carbon. An estimation of the percentage total organic carbon (% TOC) and percentage carbonate carbon (% CC) was obtained by loss on ignition at 500 °C and 1000 °C respectively (see Appendix 1). Weight loss on ignition at 1000 °C was observed to have a positive correlation with carbonate yield from isotopic analysis and therefore suffices as a reasonably good estimate of percentage carbonate. Determination of total organic content by loss on ignition may provide a reliable estimate in recent sediments. However, it is an inaccurate measure in their lithified counterparts, particularly those with relatively low organic carbon contents.

The primary isotopic composition of organic carbon usually displays the same trends as the primary carbonate signal. Therefore organic carbon analysis should be performed in any isotopic study (Knoll et al., 1986). Pell (1989) and Jansyn (1990) showed that the organic carbon content of the Wonoka Formation in the Flinders Ranges was extremely low ($\leq$ 0.22 %TOC). Pell (1989) performed six isotopic analyses on the Wonoka and Billy Springs Formation from the northern Flinders Ranges and found that $\delta\,^{13}C_{org}$ ranged between -18.94 and -29.19‰. Both Pell (1989) and Jansyn (1990) concluded that the Wonoka Formation samples probably showed thermally altered organic carbon values. Therefore due to the low organic content (sample: 086 TOC = 0.006%) and the probability of metamorphic effects, carbon isotopic analysis of the kerogen fraction was not attempted in this study.

Mineralogy of samples was determined by x-ray diffraction spectrometry as in Appendix 1. Percent mineralogical constituents was estimated from principal x-ray diffraction peaks (Royse et al., 1971 and Brasier et al., 1990) and the results presented in Appendix 2. The accuracy of method is questioned as petrographic estimates by Haines (1987) yielded much higher feldspar values. The samples were allotted to groups according to their carbonate mineralogy as follows:

< 10% dolomite = calcite

>10% dolomite = mixed calcite/dolomite

> 85% dolomite = dolomite.

All samples from the Pichi Richi field area had either mixed dolomite / calcite or 'pure' calcite mineralogy.

4.3 Stable Carbon and Oxygen Isotope Analysis

Carbon and oxygen have two stable isotopes: ^{12}C, ^{13}C and ^{16}O, ^{18}O respectively. These isotopes may reside in one of several different reservoirs of the earths hydrological and biological systems. Fractionation between the two isotopes of each element occurs due to slight differences in reactivity (Anderson and Arthur, 1983). Physicochemical and biochemical fractionation of the isotopes usually occurs during transfer between the oxidised (bicarbonate) and reduced (organic)carbon reservoirs and the atmospheric and oceanic oxygen reservoirs. Changes in the isotopic composition of the reservoirs occurs when a significant amount of one isotope is locked up in one particular reservoir. Therefore the isotopic composition of any one reservoir is the result of the balance between itself and other sinks.

The isotopic fractionation of carbon is not temperature dependent (Anderson and Arthur, 1983). Rather the major cause of carbon isotopic fractionation is photosynthesis which results in the preferential uptake of ^{12}C into organic matter. Hence, the carbon isotopic composition of seawater is controlled by the mass balance between the reduced (organic) carbon and the oxidised (bicarbonate) carbon. Relative changes in the preservation of organic carbon or recycling of biogenic carbon dioxide causes excursions in the carbon isotope signatures of both reservoirs. Secular variation in these carbon isotope signals has been attributed to various local and global phenomena, including basin restriction (Knoll et al., 1986), organic burial (Schidlowski, 1988), productivity (Magaritz, 1990), and biomass change and mass extinctions (Magaritz, 1989)

The isotopic composition of oxygen on the other hand is highly temperature dependent. Therefore physical processes such as evaporation play an important role in determining the isotopic composition of the oxygen reservoirs. Vapours of oxygen are usually enriched in the light oxygen isotope. As a result, meteoric water is highly negative with respect to the major reservoir, seawater. During glacial periods, preferential uptake and storage of the light isotope in glacial ice causes a reciprocal positive isotopic excursion in the oxygen isotope signal of marine carbonates. Oxygen isotopes therefore have been used extensively in palaeoclimatic studies.

The isotopic composition of carbonate reflects the fluid from which it is precipitated. Therefore the primary isotopic composition of marine carbonate rocks documents the secular variation in the isotopic composition of seawater throughout the geological record. The isotopic composition of carbonate is reported in $\delta^{13}C$ or $\delta^{18}O$ notation according to the equations:

$$\delta\,^{13}C = \frac{^{13}C / ^{12}C \text{ sample} - ^{13}C / ^{12}C \text{ standard}}{^{13}C / ^{12}C \text{ standard}} \times 1000$$

$$\delta\,^{18}O = \frac{^{18}O / ^{16}O \text{ sample} - ^{18}O / ^{16}O \text{ standard}}{^{18}O / ^{16}O \text{ standard}} \times 1000$$

The results are usually reported in parts per thousand (‰) relative to the Pee Dee Belemnite (PDB) standard.

Carbon and oxygen isotopic analyses were performed on whole-rock samples of the Wonoka Formation canyon and carbonate platform sequences. Drilled aliquots of sample were reacted according to the carbonate mineralogy as determined by XRD (Appendix 1). Calcite samples (< 10 % dolomite) were reacted at 25 °C overnight. Mixed calcite-dolomite samples (10 - 85 % dolomite) were reacted at 25 °C for half an hour and at 50 °C overnight to release the carbon dioxide from calcite and dolomite, respectively.The results of all isotopic analyses are shown in Appendix 2.

4.3.1Canyon Data

The Pichi Richi South, Richman Valley and Waukarie Creek sections all represent lower canyon fill. With the exception of the wallplaster the isotopic data of the canyon fill is very homogeneous: $\delta^{13}C$ = -8.5 to -7.0 and $\delta^{18}0$ = -17.2 to -13.0 ‰ PDB (Fig. 4). The homogeneity of the isotopic signal is highlighted in the plot of isotopic composition versus stratigraphic height (Figure 4).

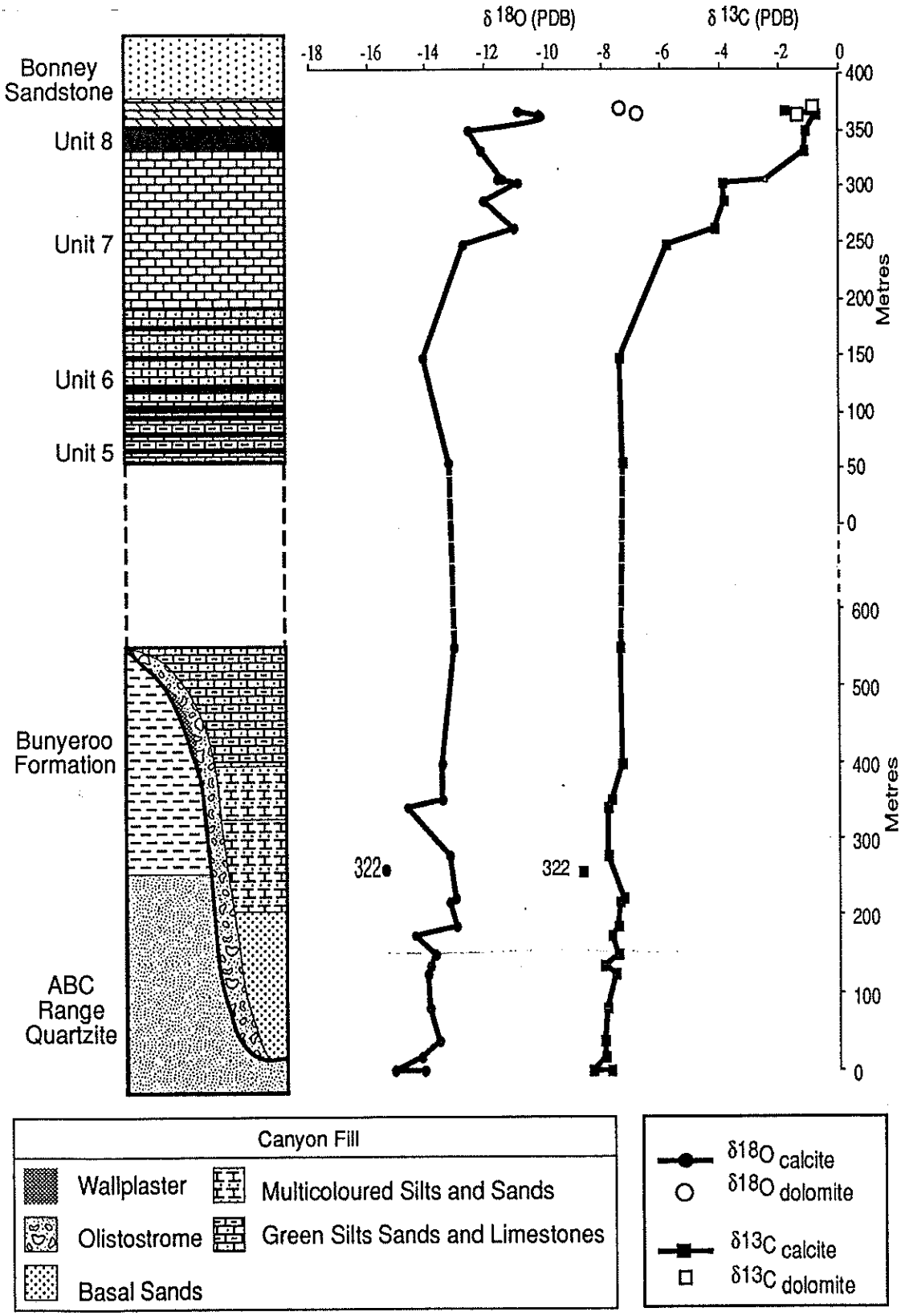

Figure 4: Composite carbon and oxygen isotope curve for the Late Proterozoic Wonoka Formation canyon and carbonate ramp sequences Sample 322 Wallplaster from Waukarie Creek Canyon.

At Waukarie Creek the lowest canyon unit sampled , the wallplaster, (975-322) has isotope values of $\delta^{13}C$ = -8.90 and $\delta^{18}O$ = -17.14‰ PDB respectively. These isotope values correspond closely to those values obtained by Eickoff et al (1988) which were $\delta^{13}C$ = -8.9 and $\delta^{18}0$ = -15.4‰. A cross plot of $\delta^{13}C$ and $\delta^{18}0$ data from the Wonoka Formation is presented in Figure 5. It is observed from this that there is a strong covariation between carbon and oxygen from the Wonoka Formation. A calcite vein from the Pichi Richi South canyon was analysed and found to be isotopically similar to the host rock ($\delta^{13}C$ = -7.3 and $\delta^{18}O$ = -13.9‰).

4.3.3 Carbonate Platform Data

The Devils Peak section represents the carbonate platform sequence of the Wonoka Formation in the Pichi Richi study area. As seen in Figure 4 the $\delta^{13}C$ values from the platform sequence delineate a major positive excursion from -7.5 to -0.5‰. Although not as distinct as the carbon trend, oxygen isotopes show a similar increase in isotopic values up section (Figure 4) . In the lower part of the platform sequence isotopic values are similar to those of the canyon sequence ($\delta^{13}C$ = -7.0 to -8.0 and $\delta^{18}O$ = -13.0 to -14.0‰). Up sequence the isotopic ratios increase to a maximum value of $\delta^{13}C$ = -0.5 and $\delta^{18}O$ = -7.5‰. A calcite vein from the lower platform sequence isotopic value was $\delta^{13}C$ = -7.68 and $\delta^{18}O$ = -13.52 ‰ respectively, which is similar to the surrounding rocks and the veins in the Pichi Richi South canyon sequence.

The isotopic value for the mixed calcite / dolomite samples at the top of the Devils Peak section showed no significant difference in carbon isotopic composition. However, a considerable differnces of 3‰ was observed in their oxygen isotopic composition (dolomite $\delta^{18}O$ = -7.0 and calcite $\delta^{18}O$ = -10.4). Therefore oxygen isotopic composition varies according to carbonate mineralogy.

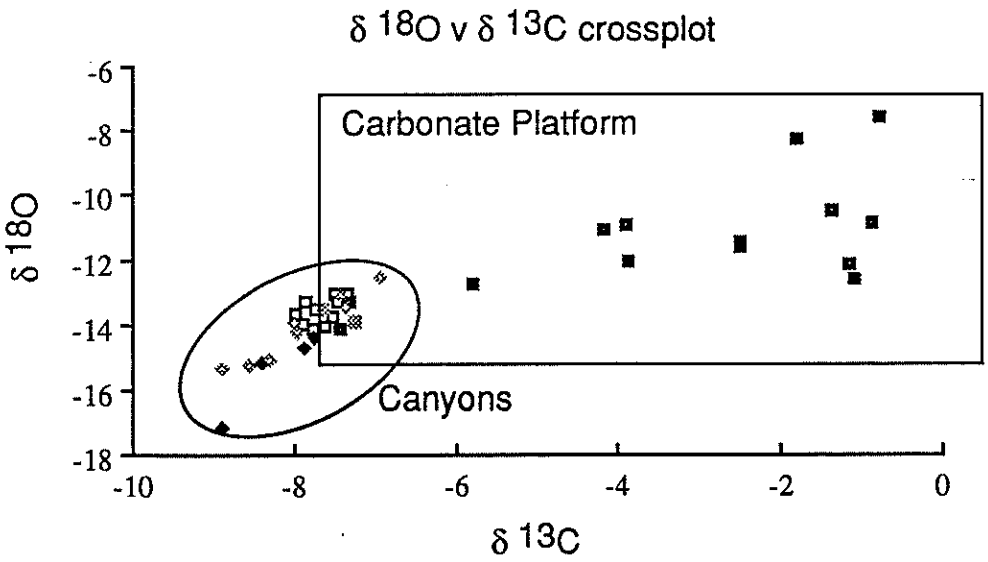

Figure 5: Crosspot of $\delta^{18}O$ versus $\delta^{13}C$ for canyon and carbonate platform data. Note strong covariation between carbon and oxygen.

4.3.3 Interpretation of the Carbon and Oxygen Isotope Record

The use of carbon and oxygen isotopes in both intra- and inter-basinal correlation requires comparison with other established and published data from almost identical strata of the same age. As previously noted Eickoff et al (1988) found carbon and oxygen isotope values for the wallplaster and clasts from the Wonoka Formation canyon sequence that are very similar to those obtained in the present study. Jansyn (1990) and Urlwin (1992) also recently reported similar isotopic profiles from the Wonoka Formation at the Bunyeroo Gorge type section and the Warraweena area which is (Copley 1:250 000 Sheet) approximately 80 km to the north of Bunyeroo Gorge.

The correlation between the carbon isotopic data from other investigations and a composite carbon isotope curve, compiled using the canyon and platform data is shown in Figure 6. The same positive excursions observed in the Pichi Richi region correlates across the basin . The trend from highly negative values in units 3-6 ($\delta^{13}C$ = -8 to -7‰) is followed by a pronounced positive swing ($\delta^{13}C$ =-6 to -0.5‰) in units7 and 8. The upper units of the Wonoka Formation continue this positive excursion to high positive values $\delta^{13}C$ values in the range +4 to+6‰ (Urlwin, 1992).

Numerous authors have proposed that canyon incision occurred sometime during deposition of unit 3 (von der Borch et al., 1982,1985,1989; Haines,1987; Eickoff et al., 1988; Christie Blick et al., 1990). Isotopic similarities between the canyon fill of this study, and units 3 - 5 of the carbonate platform (Jansyn 1990; Urlwin 1992) also suggest that incision of the Wonoka canyons was coeval with deposition of unit 3. The isotopic signal of the middle Wonoka Formation does not seem to be affected by facies change because, both the canyons and the carbonate platform sequences have similar isotope profiles.

The Wonoka Formation carbonates are highly depleted in both ^{18}O and ^{13}C. The carbon isotopic composition of Proterozoic and Phanerozoic marine carbonates are relatively conservative, varying between plus and minus three (Degens, 1971). A trend towards more negative isotopic values with increasing age has been observed throughout the geologic record (Hudson, 1975, 1977). This trend has been attributed to diagenetic or metamorphic alteration, or a difference in the chemistry of Proterozoic seawater.

FIGURE 6: INTRA-BASINAL STRATIGRAPHIC AND ISOTOPIC CORRELATION OF THE LATE PROTEROZOIC WONOKA FORMATION

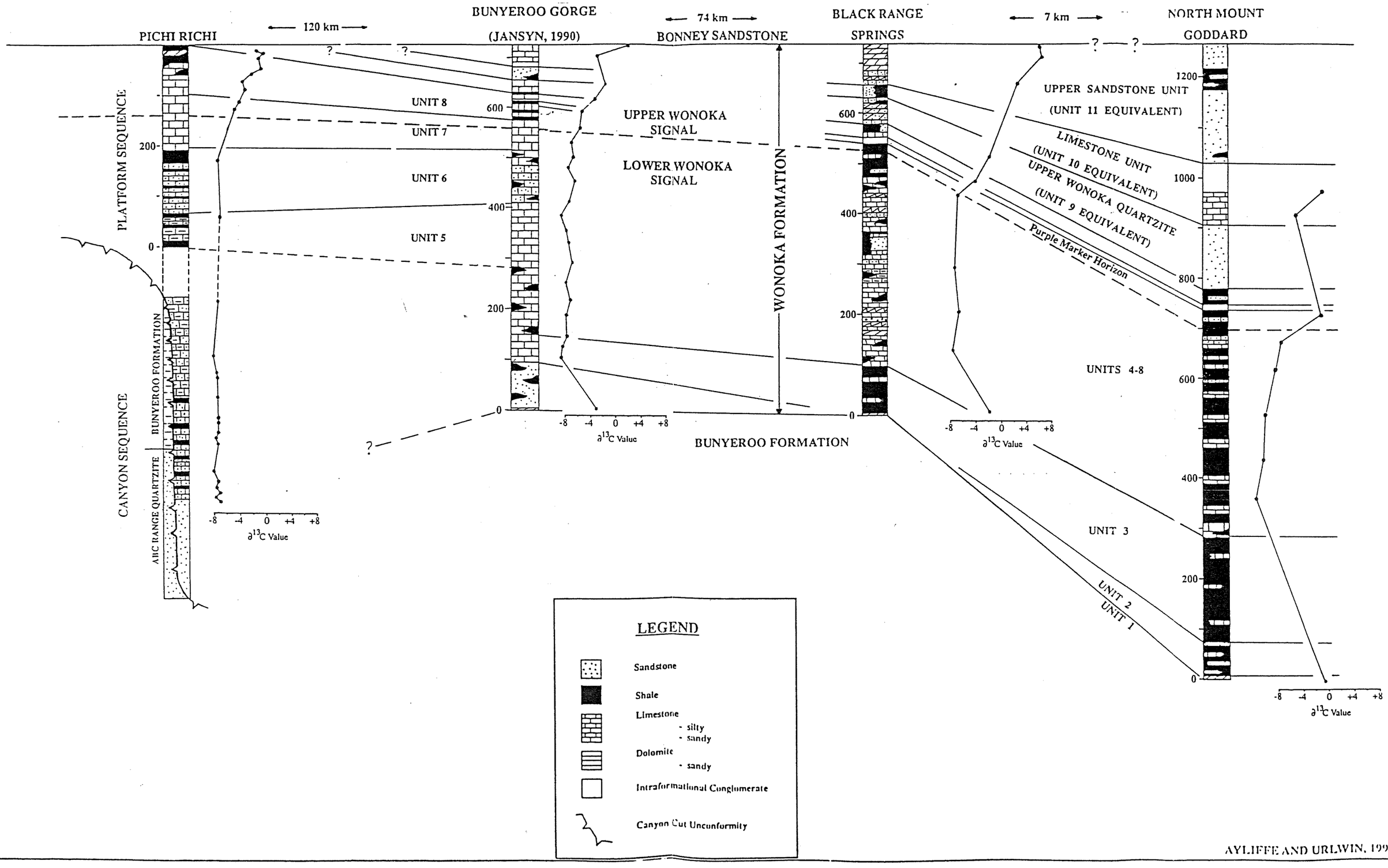

AYLIFFE AND URLWIN, 1992

A review of the literature for rocks of late Vendian age with similar isotopic values to the Wonoka Formation does not support a primary isotopic signal. Typical strata of late Proterozoic (Vendian) age fall within the range $\delta^{13}C = \pm 6$ ‰ with most having normal marine values $\delta^{13}C = \pm 3$‰ (Brasier et al.,1990, Kaufman et al., 1991, Knoll,1991, Lambert and Donnelly, 1991, Brasier, 1992, Brasier et al., 1992). Possible reasons for the discrepancy between the highly negative values obtained for the Wonoka Formation in this study and other late Proterozoic strata are bacterial oxidation of organic matter, and / or incipient metamorphism of kerogen.

Irwin and Curtis (1977) attributed highly negative carbon isotopic values to bacterial degradation of organic matter. The reworking of organic matter by sulphate reducing bacteria during early diagenesis returns ^{12}C back into the water column which in restricted basin environments may lead to highly negative carbonate $\delta^{13}C$ values (Knoll et al.,1986). Kerogens isolated from late Proterozoic sediments in the Pichi Richi region have maturation levels typical of the zone of metagenesis (atomic H/C ratios ~ 0.3; equivalent vitrinite reflectance ~ 2.5%: D. M. McKirdy, pers. comm.) Therefore any organic matter in the Wonoka Formation probably has undergone thermally induced decarboxylation which could produce carbonate cements with highly negative carbon isotopes. However, these processes are unlikely to have affected the Wonoka Formation greatly due to its low organic carbon content (Pell, 1989; Jansyn, 1990)

Brasier et al (1992) attributed carbon and oxygen isotope values such as those recorded in the Wonoka Formation ($\delta^{13}C$ = -7 to -8‰ and $\delta^{18}O$ = -15 to -17.4‰) to metamorphism and granitic intrusion. Carbon dioxide distillation during medium to high grade metamorphism depletes carbonates in ^{13}C and ^{18}O to produce highly negative carbon and oxygen isotopes values (McNaughton and Withnall, 1985). The similarity between the isotopic values of the calcite veins which are Delamerian in age and the host is possible evidence for some resetting of the oxygen isotope signal but the effect of the orogeny on the carbon isotope signal remains uncertain.

Oxygen isotopes change in response to metamophism due to their temperature dependence and therefore are useful indicators of the maximum temperature to which sediments have been exposed. The highly negative oxygen isotopes values of the Wonoka Formation ($\delta^{18}O$ = -17.0 to -10.0‰) reflect burial temperatures rather than the primary isotopic composition of seawater.

Thus, assuming a isotopic composition for late Proterozoic seawater equal to present day ($\delta^{18}O$ = -0.5‰ ±3.0 SMOW), and using equation 1, (from Arthur and Anderson 1983), burial temperatures for the Wonoka Formation can be calculated.

$$t\ (°C) = 16.9 - 4.2(\delta c - \delta w) + 0.13(\delta c - \delta w)^2 \qquad \textbf{(Equation 1)}$$

Where the oxygen isotopic composition of carbonate δc = PDB and seawater δw = SMOW (Anderson and Arthur 1983).

The calculated burial temperatures for the Wonoka Formation range between 100 and 125 °C depending upon the assumed primary isotopic composition of seawater and the $\delta^{18}O$ value used for the Wonoka Formation. These temperatures are equivalent to approximately 5km of burial with an assumed geothermal gradient of 2-3 °C per 100m and correspond well with the approximate thickness of the overlying latest Precambrian and Cambrian sediments of the Adelaide Geosyncline (5km).

The predicted burial temperatures for Wonoka Formation are supported reasonably by the estimated vitrinite reflectance of approximately 2.5 for the Wonoka Formation at Depot Creek. Assuming an effective heating time of 80 million years (age of the Wonoka Formation, 580 million years minus age of the Delamerian Orogeny, 500 million years) this corresponds to a maximum burial temperature between approximately 165 to 180 °C.

The moderately high burial temperature and estimated vitrinite reflectance of the Wonoka Formation probably reflects the effects of deep burial and metamorphism during the Delamerian Orogeny. The isotope values of calcite veins which formed during the orogeny is evidence that the oxygen isotopes have been reset subsequent to deposition. Alteration of the carbon isotopic signal is dependent upon the water rock ratio and preservation potential of the strata (Marshall,1990). Therefore pure micritic carbonates which have undergone diagenesis with a low water / rock ratio will most likely retain the primary signal.

The highly consistent carbon isotopic trends of the Wonoka Formation throughout the Adelaide Geosyncline suggests that the carbon isotope signal is primary. Recent work in central Australia and North America reveals similar $\delta^{13}C$ values (-7 to -11‰) in certain other late Proterozoic carbonates also suggests that values of the Wonoka Formation are is primary (R.J.F. Jenkins pers. comm.) If these carbon isotope values are indeed primary, they reflect a considerable difference in the isotopic

composition of seawater during deposition of the Wonoka Formation, and / or a possibly unique geological setting for the Wonoka Formation.

One possible scenario for a geological setting capable of producing such a primary carbon isotopic signal for the Wonoka Formation has been proposed by R.J.F. Jenkins (pers comm.) In this model, gradual warming of the ocean surface water and sinking of cold dense glacial melt-water causes the ocean to become stratified (Figure 7 Postglacial). In the surface layers high productivity due to nutrient input preferentially withdraws ^{12}C from the water column whilst enriching the surface waters in the heavy isotope (^{13}C). A high flux of organic matter to the deep ocean is oxidised aerobic bacteria. The oxidation of organic matter causes the deep of the stratified ocean to become extremely enriched in dissolved ^{13}C; depleted biogenic carbon dioxide (CO_2 is 60 times more soluble in the cold deep water compared to surface water).

Therefore, during the deposition of unit 2 to lower unit 7 (basin and canyon fill sequences), the carbonate shows the ^{12}C-enriched deep bottom water carbon isotope signal. As the Wonoka Basin shallows there is a progressive increase in ^{13}C content of the carbonates deposited in the photic zone on the carbonate platform. The absence of organic-rich strata within the Wonoka Formation is strong evidence that the Wonoka Formation was deposited in oxidising conditions.

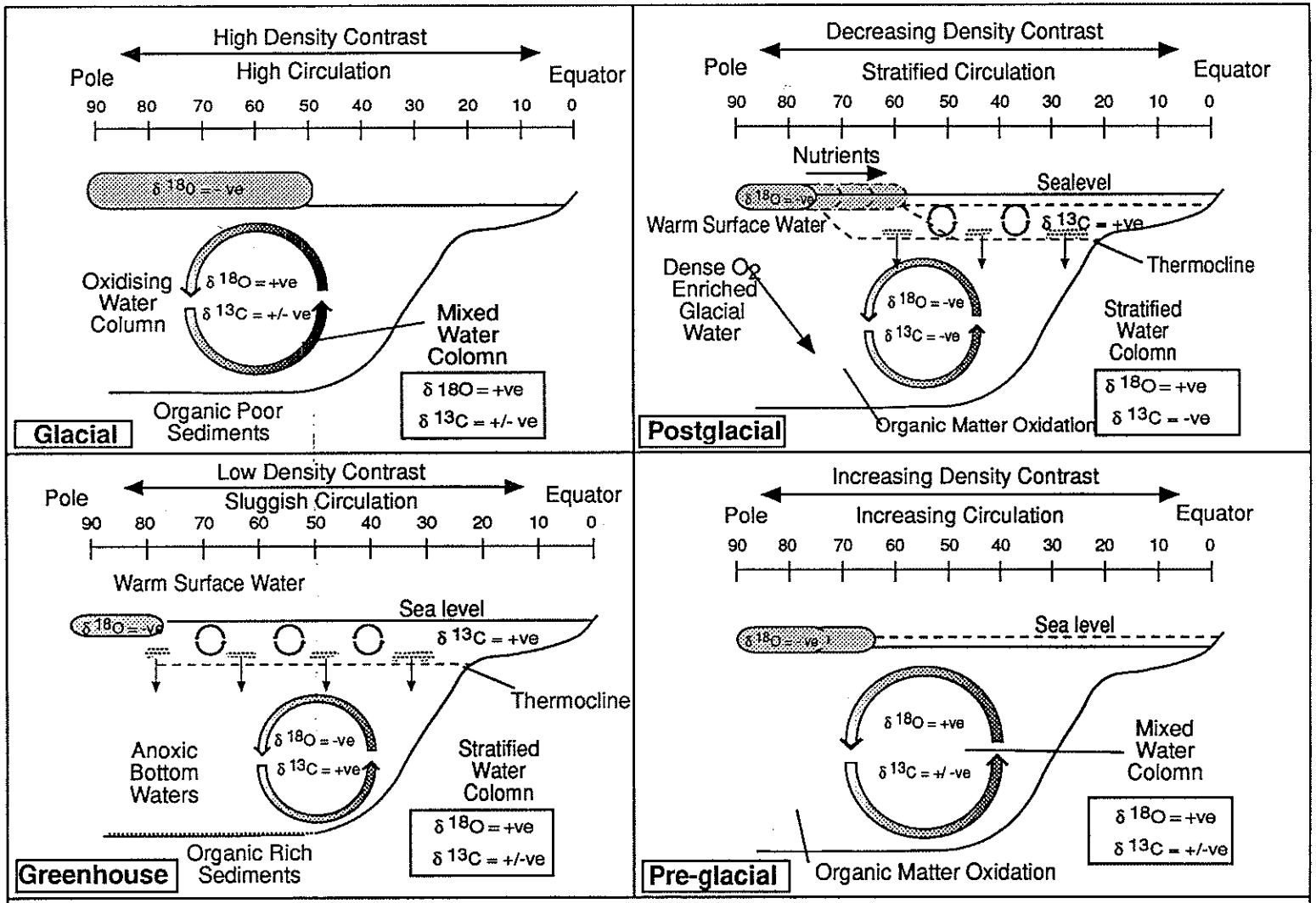

Figure 7: Proposed model for primay isotopic composition for the Wonoka Formation. Post glacial carbonate are characterised by highly negative carbon isotope signal similar to the Wonoka Formation (based on ideas of R.J.F. Jenkins 1992).

4.4 Strontium Isotope Geochemistry

4.4.1 Introduction

Strontium has four isotopes ^{84}Sr, ^{86}Sr, ^{87}Sr and ^{88}Sr. This, and the fact that strontium is incorporated into the carbonate crystal lattice, makes it a useful tool in isotope stratigraphy. However only ^{87}Sr and ^{86}Sr are used in strontium isotope stratigraphy. Strontium 87 is derived from the radioactive decay of ^{87}Rb. As a result there is a steady increase in the ^{87}Sr / ^{86}Sr ratio in rocks containing ^{87}Rb.

The strontium isotopic composition of carbonates directly reflects the solution from which they were precipitated without fractionation. The isotopic composition of strontium in seawater will therefore be recorded in the isotopic signature of ancient carbonate rocks. The composition of seawater is the result of inputs of strontium from several sources. Low ^{87}Sr / ^{86}Sr values are derived from the input of hydrothermal and volcanic sources. On the other hand, high ^{87}Sr / ^{86}Sr ratios reflect the weathering of old cratonic rocks where rubidium has had time to decay. Ancient marine carbonates usually have an intermediate strontium isotopic composition compared to these two end members.

The strontium isotopic composition of Proterozoic carbonates (and therefore seawater) shows a significant increase in ^{87}Sr / ^{86}Sr through time. This increase in the isotopic composition is due to intense tectonic activity, the steady decay of rubidium, and the absence of the buffering effect of carbonates (Faure 1986, Veizer 1983). In contrast the strontium isotopic composition of carbonates from the Phanerozoic rock record is conservative, fluctuating between a low of 0.7068 and a high of 0.7091. This is due to the buffering influence of previously deposited carbonates and a decrease in tectonic activity. The isotopic composition of seawater for the late Proterozoic is shown in Figure 8

4.4.2 Strontium Isotope Analysis

Strontium isotopic analysis was performed on the carbonate portion of six samples of the Wonoka Formation three from the Pichi Richi South canyon and three from the Devils Peak platform sequences. Analyses were performed according to the methods as outlined in Appendix 1. The resulting data are presented in Appendix 1 and summarized below in Table 1.

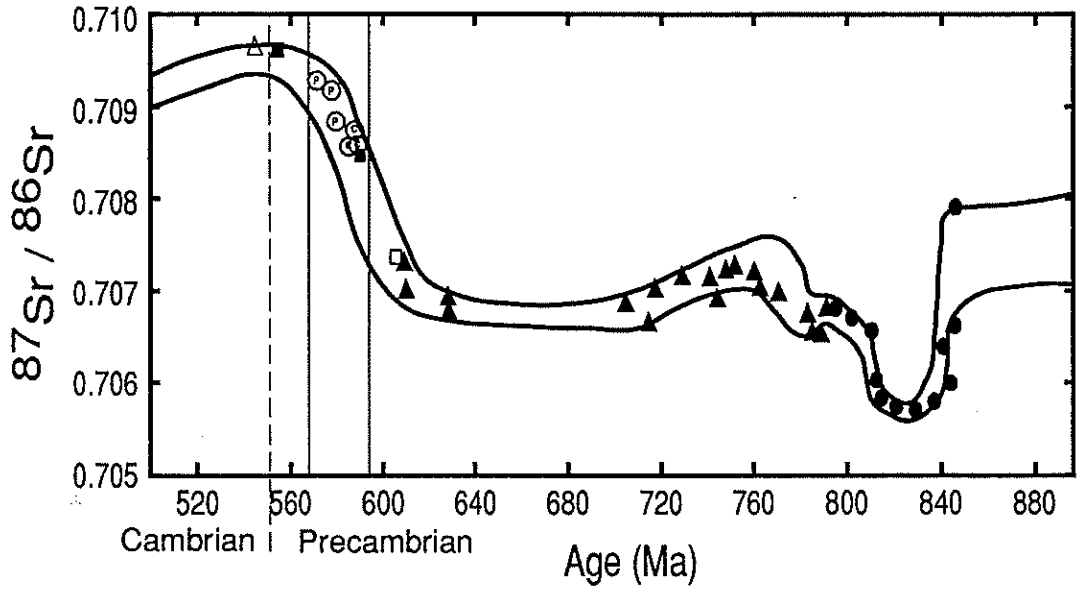

Figure 8: Late Proterozoic seawater $^{87}Sr/^{86}Sr$ isotopic composition adapted from Asmerom et al., (1991). Filled symbols from Asmeron et al., (1991), open squares Trezona Formation, open triangles Wilkawillina Limestone from Singh (1986) and open circles Wonoka Formation (carbonate platform -P, canyon-C).

Canyon	$^{87}Sr / ^{86}Sr$	Platform	$^{87}Sr / ^{86}Sr$
975-010	0.708555	975-086C	0.708672
975-038	0.708669	975-098	0.710130
975-062	0.709114	975-115	0.709308

Table 1: Strontium isotopic compositiopn of the late Proterozoic Wonoka Formation canyon and carbonate platform sequences Pichi Richi Pass, Southern Flinders Ranges.

4.4.3 Strontium Isotopic Data

With the exception of sample 975-086c the canyon section has much lower strontium isotope values than does the Devils Peak section. This is possibly due to the input of heavy, terrestrially derived strontium during meteoric diagenesis of the carbonate platform. Derry et al (1989) state that the lowest strontium isotope value of marine carbonates best reflect the primary isotopic composition of the ancient seawater from which they were deposited. Therefore using this reasoning the best estimate of the strontium isotopic composition for seawater during Wonoka Formation deposition is approximately 0.708555 to 0.70870.

These values correspond and plot within the range of those obtained from the Trezona Formation (0.7071and 0.7085) and Wilkawillina Limestone (0.7095) by Singh (1986). Urlwin (pers comm) has reported 0.70936 and 0.70968 for the upper Wonoka Formation which are slightly greater than those values obtained from the Devils Peak carbonate platform section. A composite strontium isotope curve which shows isotopic variation with stratigraphic height is shown in Figure 9: The strontium isotopic composition of the Wonoka Formation corresponds well with published late Proterozoic seawater curves (Fig. 8 after Asmerom et al., 1991).

Like other isotope and geochemical data the primary isotopic composition of strontium is prone to alteration and therefore is a good indicator of diagenesis. Plots of strontium isotopic composition and various diagenetic tracers highlight the differences between the canyon and carbonate platform carbonates (Figures 10-13). Diagenetic alteration (particularly meteoric) usually results in an increase in the ^{87}Sr / ^{86}Sr ratio (Derry et al., 1992).Hence the least altered carbonates are those of the Wonoka canyon fill sequence.

Derry et al. (1989, 1992), Veizer (1983) and Brand and Veizer (1980, 1981) have designed geochemical methods to determine the magnitude of alteration. In this study, the least altered samples were taken to be those with no rubidium, a high strontium concentration, low Mn / Sr ratio (< 1-2) and a high Ca /Sr ratio (Figs. 10-13) (see Chapter 5). Although the relatively ^{87}Sr enriched carbonate of the platform sequence is probably altered it ^{87}Sr /^{86}Sr values still correspond well with the published strontium isotope curve. This evidence suggests that the Wonoka Formation strontium isotopes reflect a primary seawater composition.

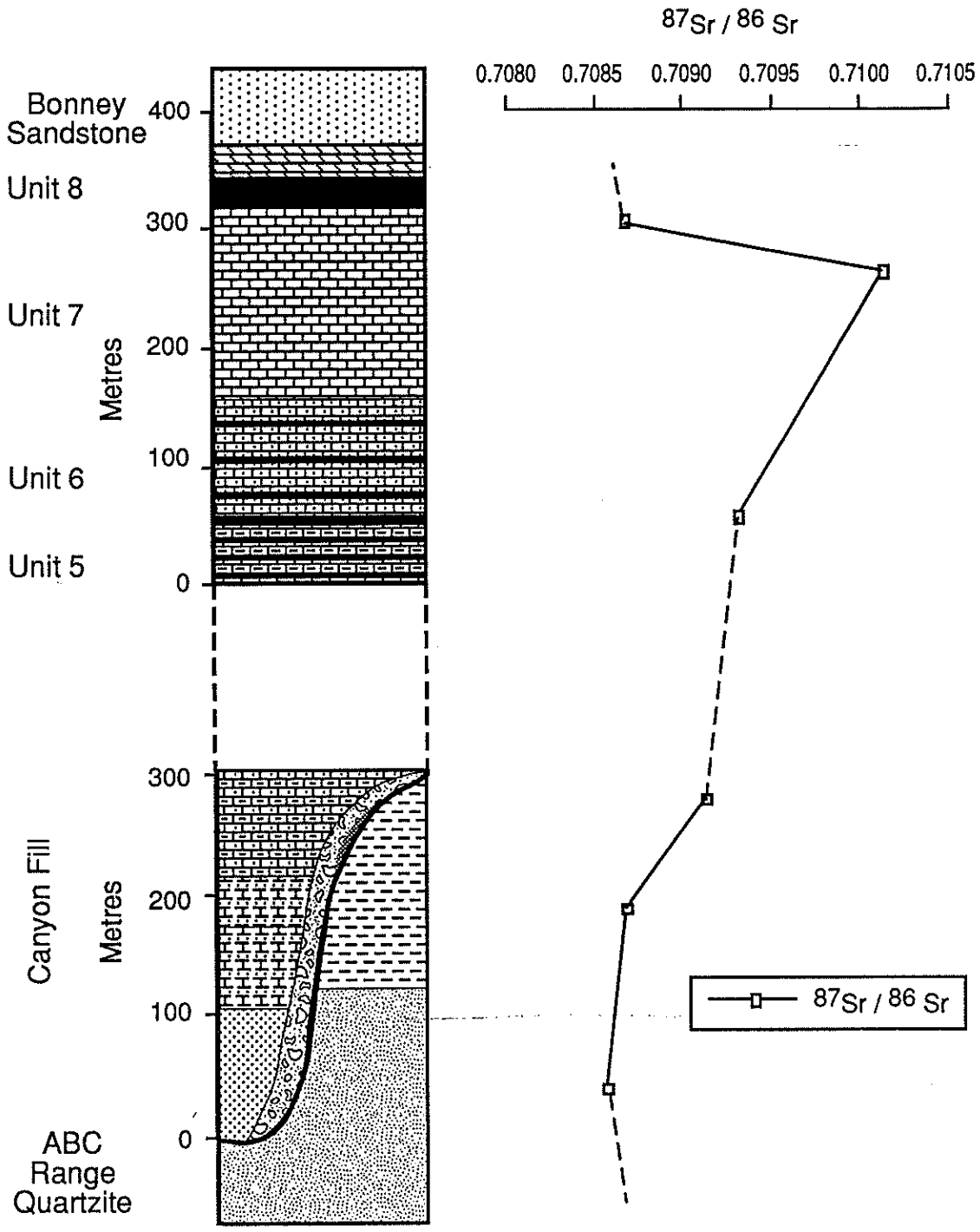

Figure 9: Composite strontium isotopic composition versus stratigraphic height for the late Proterozoic Wonoka Formation canyon and carbonate platform (See Figure 4 for canyon fill symbols) .

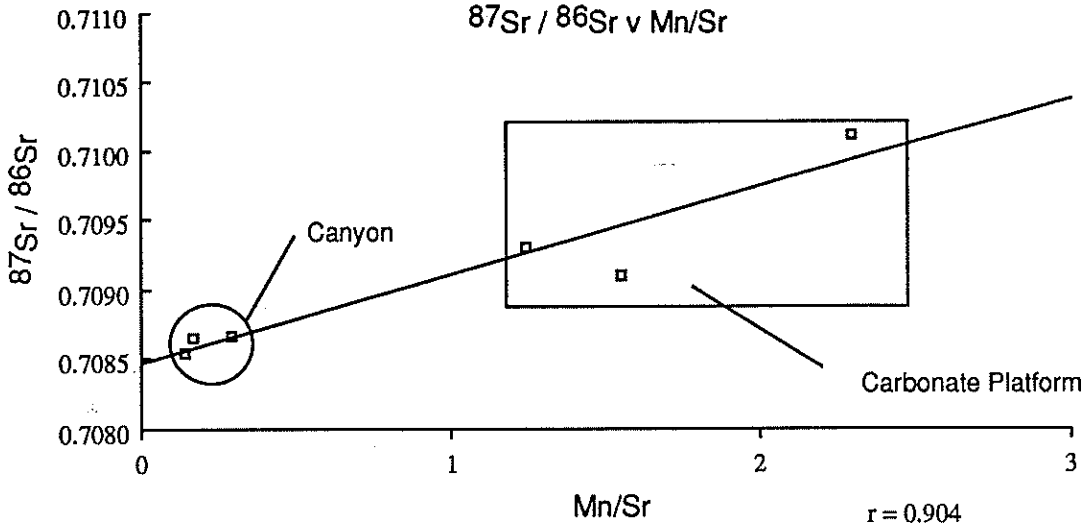

Figure 10: $^{87}Sr/^{86}Sr$ ratio versus Mn/Sr for the Wonoka Formation canyon and carbonate platform. The distinctive grouping of the two Wonoka Formation facies is probably due to differences in diagenetic history and/or the input of terrestrially derived strontium for the carbonate platform.

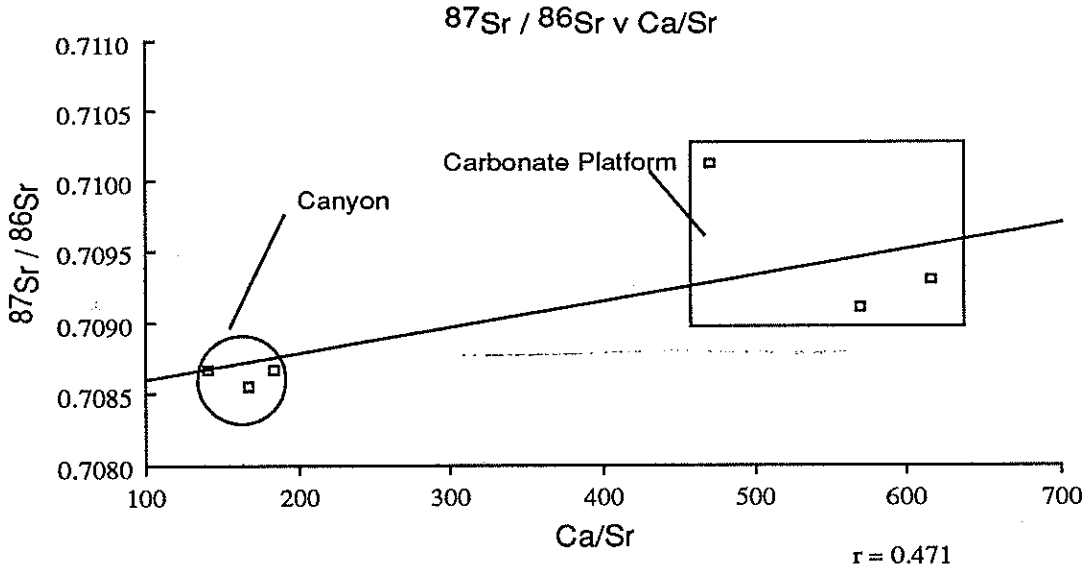

Figure 11: Strontium isotopic composition versus Ca/Sr diagenetic ratio. The relatively heavy carbonate platform $^{87}Sr / ^{86}Sr$ is possible due to the imput of terrestrially derived strontium.

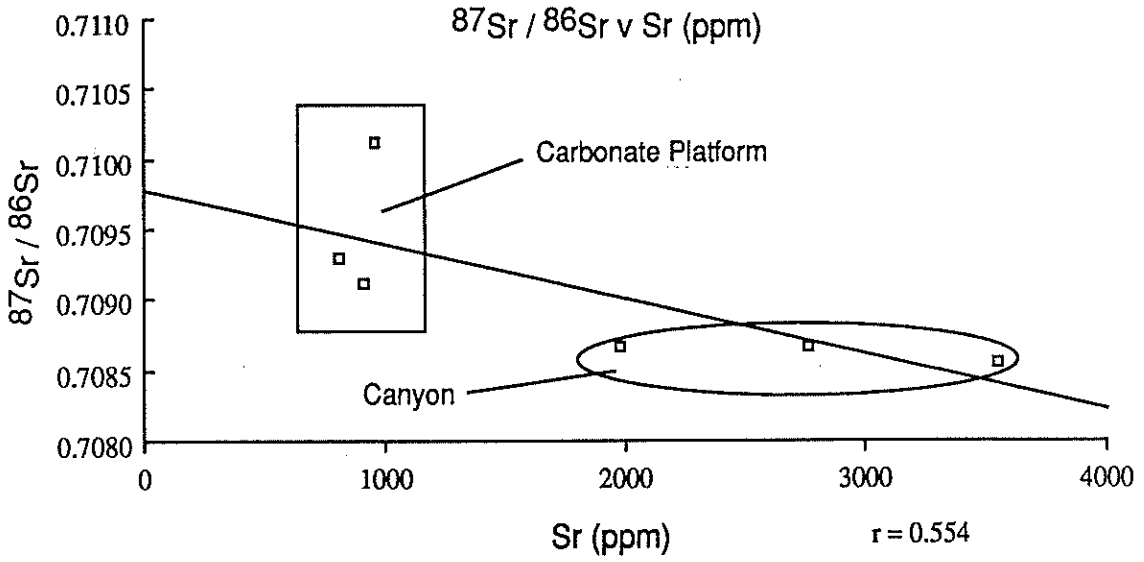

Figure 12: Carbonate platform and canyon samples $^{87}Sr / ^{86}Sr$ ratio versus strontium concentration. The canyons are characterised by high strontium content and low $^{87}Sr / ^{86}Sr$ which reflects its diagenetic history and depositional environment.

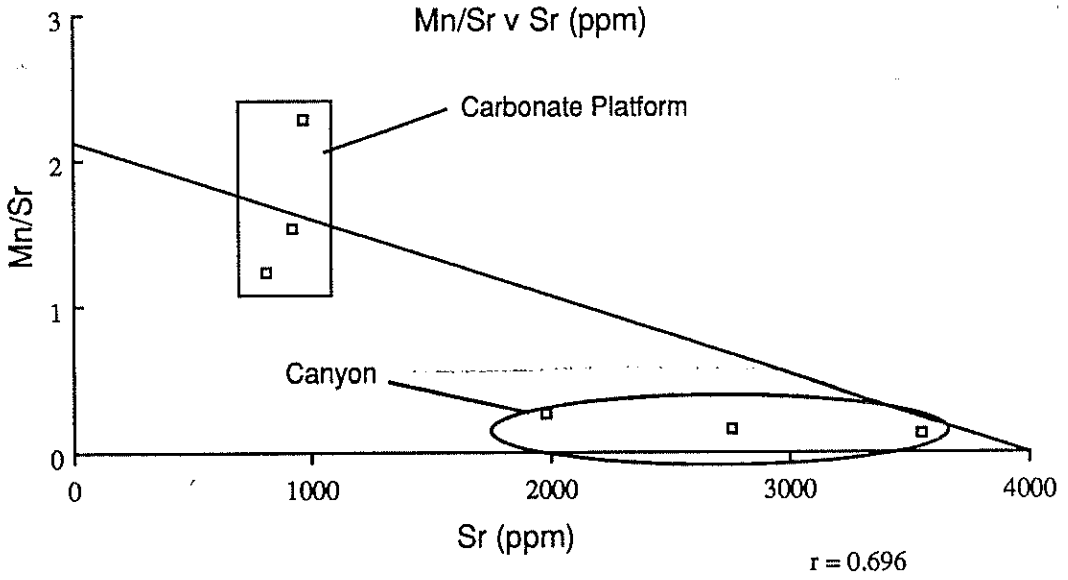

Figure 13: Inverse relationship between strontium content and Mn/Sr ratio with increasing diagenesis. Canyon samples which have relative high strontium concentration and low Mn/Sr are probably least altered compared to the carbonate platform.

4.5 Major and Trace Element Geochemical Analysis

4.5.1 Introduction

Like many other minerals, carbonates incorporate numerous cations and trace elements into their crystal structure. Whilst calcium and magnesium are the most abundant, cations like iron (Fe), sodium (Na), manganese (Mn), and strontium (Sr) may also be included in the calcite lattice. Incorporation of these trace element cations into the carbonate lattice is dependent upon the distribution coefficient of the particular element and the size and crystal structure of the carbonate phase. Consequentally cations larger the calcium (Sr, Na, Ba, and U) and are incorporated into orthorhombic aragonite and cations smaller than calcium (Mg, Fe, Mn, Zn, and Cu) into rhombohedral calcite.

Diagenesis of limestones is usually accompanied by a change in geochemistry. Derry et al. (1992) state that alteration of limestone sufficiently to affect carbon isotopic composition should be identifiable from trace element and strontium isotopic ratios. Therefore selected major and trace element concentrations were measured by atomic absorption to assess the preservation and diagenetic overprint of the selected Wonoka Formation samples. The major and trace elements of calcium, magnesium, iron, manganese, strontium and rubidum have been found to be sensitive indicators of alteration and therefore were used in this study.

4.5.2 Major and Trace Element Analysis

The carbonate portion of the sample was selectively dissolved according to the methods in Appendix 1. The samples were analysed using spectrometer and found to correlate well with major and trace element abundances obtained from iron microprobe analysis. The results of elemental abundances are presented in Appendix 2 . Selected major and trace element (atomic absorption) data for the Pichi Richi South canyon and Devils Peak carbonate platform sequences are shown in Table 2.

CANYON DATA			CARBONATE PLATFORM DATA		
Element	Range	Average	Element	Range	Average
Ca	45.7- 52.3	-	Ca	43.3-52.2	-
Mg	4200- 9400	6182	Mg	6000-20000	10711
Fe	2500-6400	4350	Fe	3800-7507	5207
Mn	384-691	656	Mn	990-2192	1396
Sr	980-3546	2028	Sr	326-957	738
Mn / Sr	-	< 1.3	Mn / Sr	-	> 1.3
Ca / Sr	-	< 550	Ca / Sr	-	> 550

Table 2: Selected major and trace element data from atomic absorption analysis. Note all data in parts per million (ppm)except Ca which is in Wt%.

4.5.3 Discussion of Major and Trace Element Geochemical Data

Several major differences in geochemistry characterize the Wonoka Formation canyon and platform sequences (Table 2). Canyon fill has high strontium (> 1000 ppm), low manganese(<700 ppm), and low magnesium (Ave. 6200 ppm) concentration. The platform sequence on the other hand has low strontium (< 1000 ppm), high manganese (> 1000 ppm) and high magnesium (Ave 10700 ppm) concentrations. These differences in trace element composition between the canyons and carbonate platform are highlighted in Figures 14-21.

The high strontium concentrations of the Wonoka Formation are indicative of neomorphism from an aragonitic precursor to low magnesium calcite (Fairchild and Spiro, 1987, Tucker, 1992, Tucker and Wright ,1990, Scoffin, 1987). Tucker (1992) has suggested that the physical and chemical conditions in the late Proterozoic ocean favoured the precipitation of aragonite. Several authors including Haines (1987), Singh (1986), Tucker (1992) and Urlwin (1992) have reported high strontium concentration from the Wonoka Formation and suggested a possible aragonitic precursor.

The higher concentration of strontium in the canyons (>1000 ppm) compared to that of the carbonate platform sequence (<1000) can be explained by differences in their depositional environment and diagenetic

history. The shallowing upward carbonate platforms sequences probably has been exposed to marine, meteoric phreatic, and vadose waters and finally burial diagenesis. The canyons on the other hand, if deposited in the deep marine environment have probably only undergone marine and burial diagenesis. Scoffin (1987) states that where aragonitic mud has undergone neomorphism in the meteoric zone strontium values may fall to approximately 200 ppm, where as in a deep marine environment aragonitic muds strontium concentration may stay as high as 1900 ppm.

Meteoric water is depleted in strontium and magnesium and enriched in manganese. Therefore during meteoric diagenesis we should observe a similar change in geochemistry. In the platform carbonates there is a decrease in strontium concentration but an increase in the magnesium composition up sequence. The increase in magnesium up sequence can be explained by penecontemperanous increase in dolomitization up sequence. Dolomite is a magnesium and manganese-rich carbonate which preferentially excludes strontium.

Other general diagenetic trends include decreasing strontium, magnesium, $\delta\ ^{18}O$ and $\delta\ ^{13}C$, and increasing iron, manganese and $^{87}Sr / ^{86}Sr$, with increasing diagenesis have been proposed by various authors including Marshall (1992), Fairchild et al., (1990) and Veizer (1983). Covaiant trends between the various diagenetic indicators can be used to show the least altered samples(Figures 14-21).

The covariant increase in manganese and iron in the calcite lattice is due to their incorporation during recrystallization at depth in a reducing environment, probably in the burial zone. The presence of iron in the calcite lattice is supported by purple/mauve staining with potassium ferricyanide and alizarin red solution (see Chapter 5). Increasing manganese at the expense of strontium has been shown to be one of the most useful diagenetic indicators (Asmerom et al., 1991, Derry et al., 1992). This conclusion is supported independently by the the increase in $^{87}Sr / ^{86}Sr$ ratio with decreasing strontium concentration

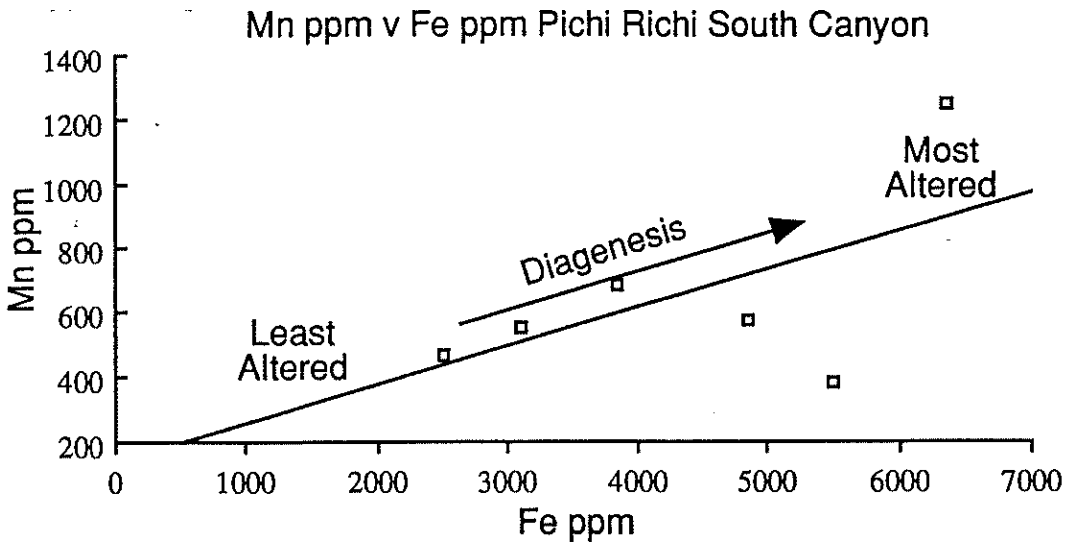

Figure 14: Trace element plot of manganese versus iron content (ppm) for the Pichi Richi South canyon sequence. Most altered sample are characterised by high manganese and iron concentrations due to their incorporation in the calcite lattice during burial zone recrystallization.

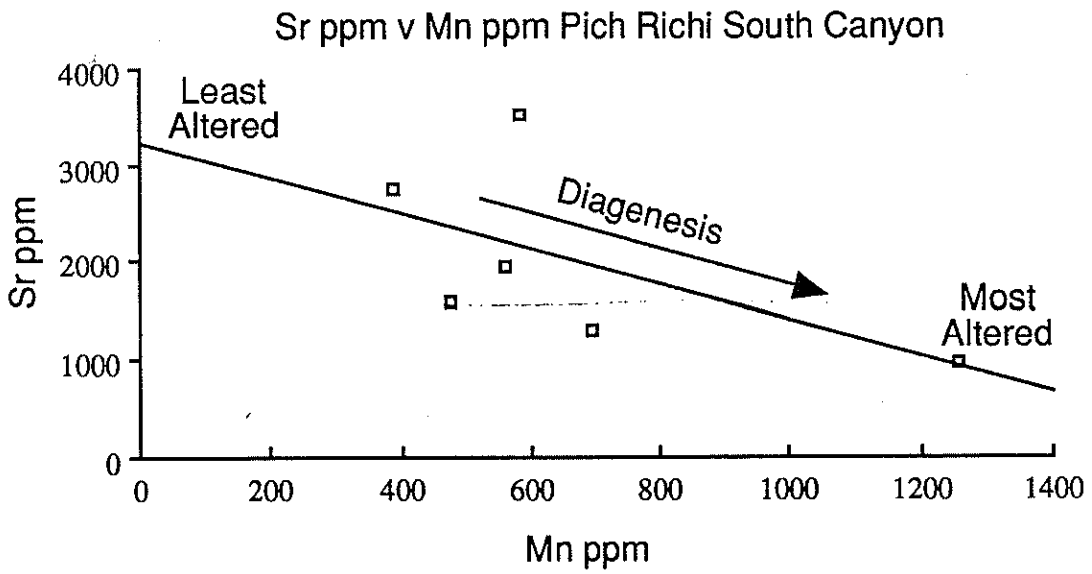

Figure 15: Diagenetic tracer strontium versus manganese for the Pichi Richi South canyon. Least altered samples have relatively high strontium and low manganese

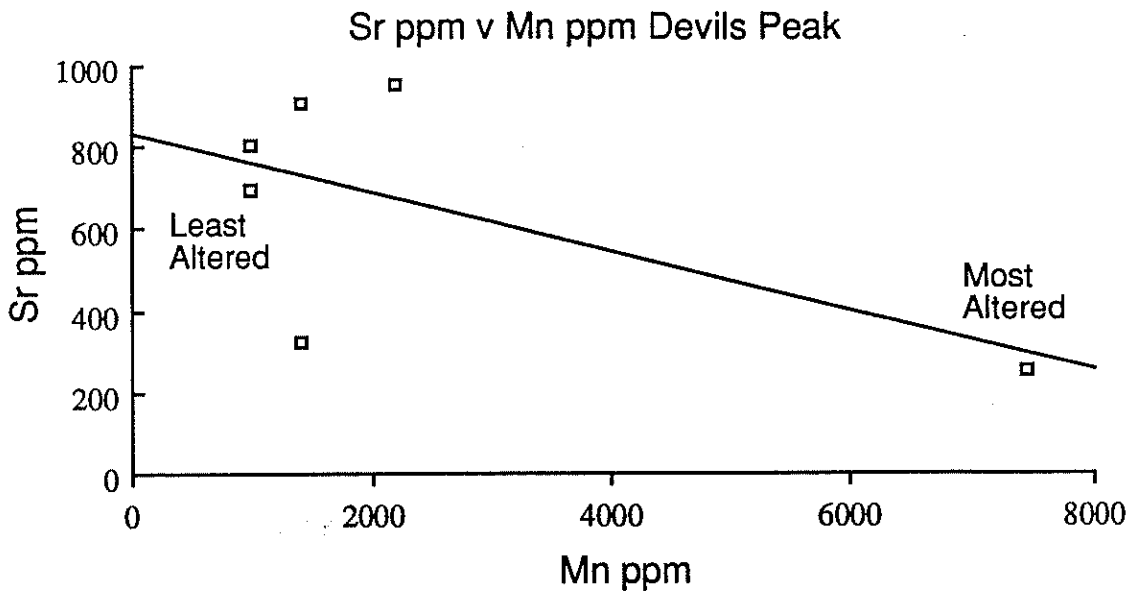

Figure 16: Devils Peak carbonate platform strontium versus manganese trace elment cross plot. Increasing diagenesis to the bottom left. Note low strontium content of the carbonate platform compared to the canyon sequence (FIgures 14 & 18)

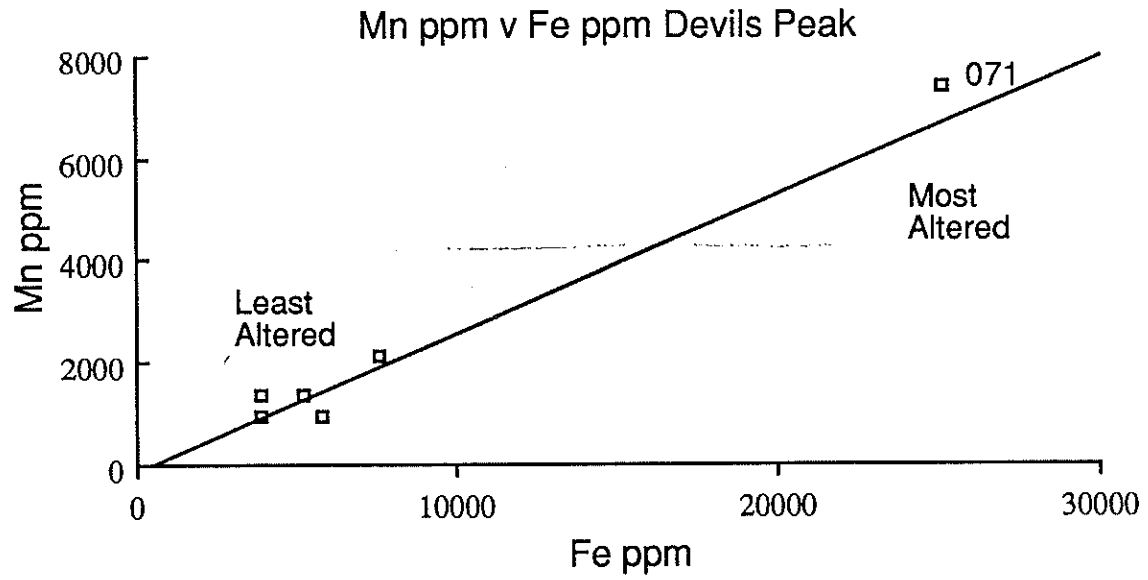

Figure 17: Covarent increase in manganese versus iron content of the Devils Peak carbonate platform samples. Sample 071 mixed dolomite calcite from the top of the Devils Peak Sequence.

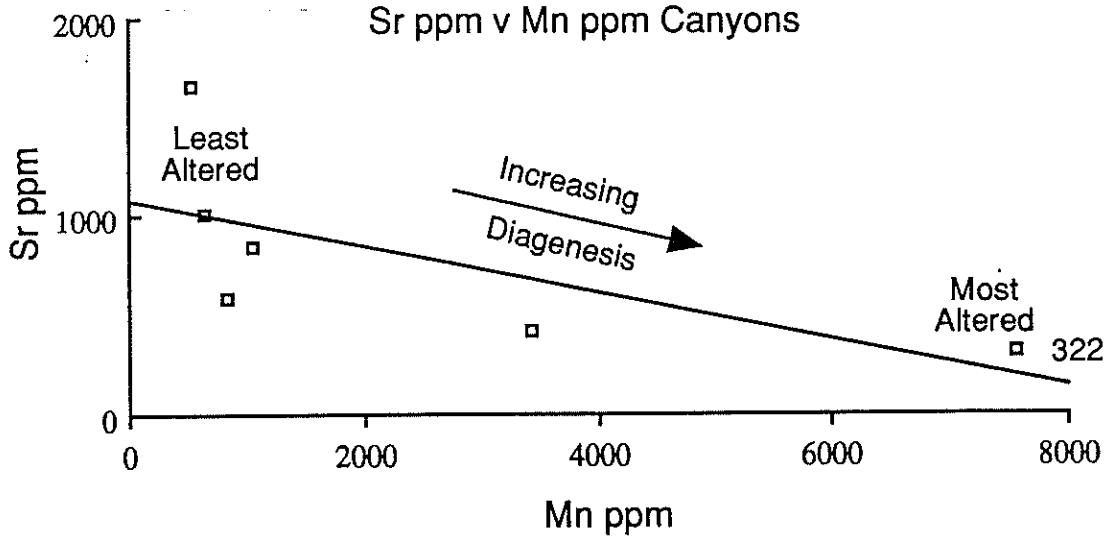

Figure 18: Inverse relationship between strontium and manganese contentof Waukarie Creek and Richman Valley canyon samples with increasing diagenesis. Sample 322 wallplaster from Waukarie Creek.

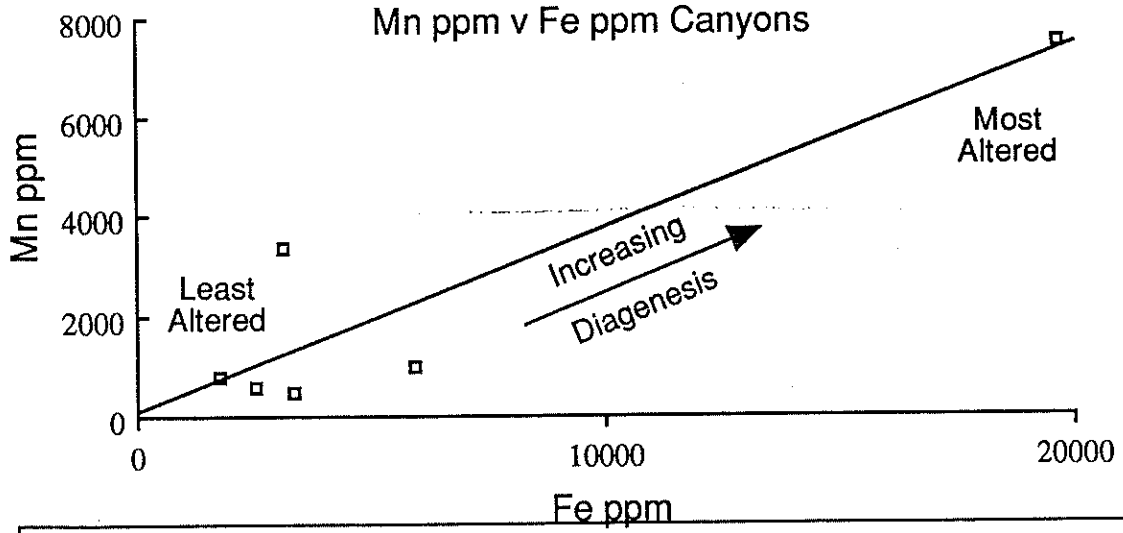

Figure 19: Waukarie Creek and Richman Valley manganese versus iron trace element plot. Canyon samples increase iron and manganese content with increasing diagenesis and alteration.

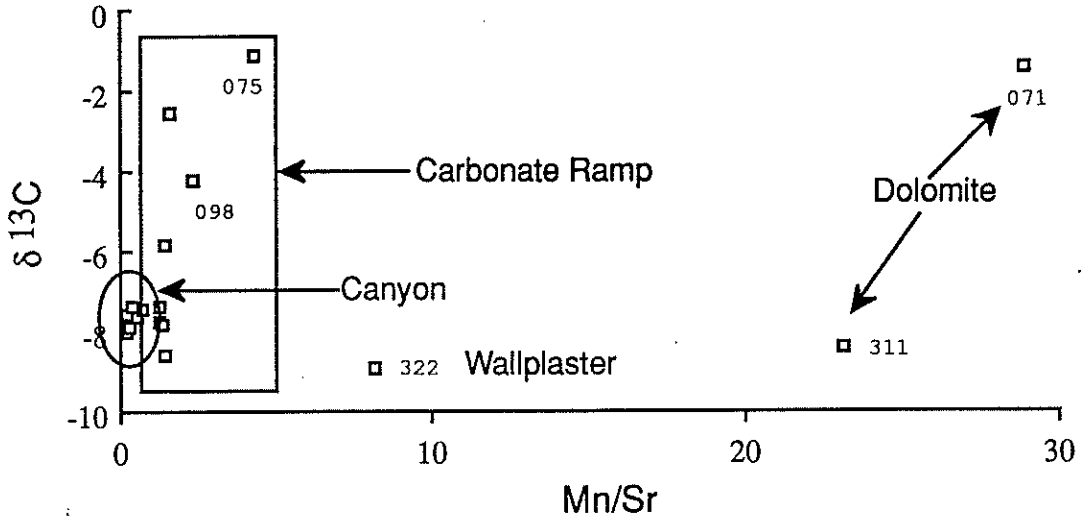

Figure 20: δ ^{13}C versus diagenetic alteration trace element parameter Mn/Sr for all isotopic analyses. Samples identified have highest dolomite component and alteration.

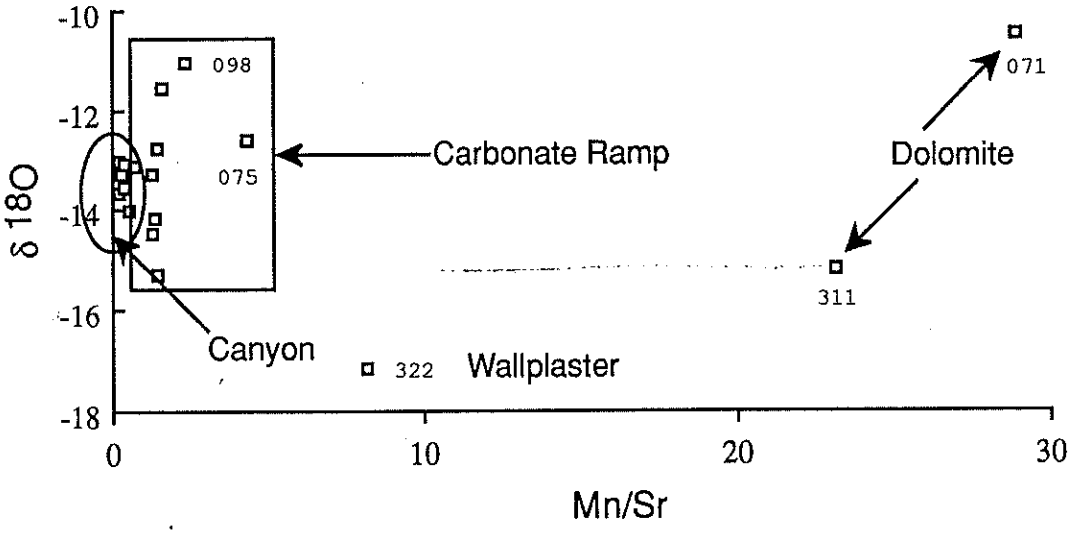

Figure 21: δ ^{18}O versus Mn/Sr ratio of the Wonoka Formation carbonate platform. Altered samples were found to have a significant dolomite component.

Chapter 5: Petrography, Diagenesis and Metamorphism

Samples from the canyon sequence are medium to fine grained sandstones and limestones (Plate 3). The detrital siliciclastics of the canyons are predominantly quartz and albite. Minor quartz overgrowths and authigenic albite are observed in thin section. The angular nature of these grains indicates possible alkaline attack by dissolved carbonate during deposition or subsequent cementation (N. Lemon, pers. comm.) The low grade metamorphism of the region has caused chlorite to replace muscovite, in shale layers of the sequence.

Clasts from the olistostrome and intraformational conglomerates were the only macroscopic allochemical detrital grains in the canyon sequence. The carbonate of the canyon sequence is therefore mostly very fine grained micrite, and carbonate cement of the medium to fine grained sandstones and limestones. The carbonate content of the canyons is determined by the proportion of siliciclastics in the rock, with carbonate-rich and carbonate-poor bands observed in hand sample and thin section. Stained thin sections and acetate peels of these carbonates show evidence of recrystallization to equant ferroan microspar (10 - 50 μm).

The carbonate of the platform sequence like that of the canyon facies is mainly carbonate cements and micrite. No allochemical components were observed except for the micritic clasts of intraformational conglomerate, although some ooids and stromatolites have been reported from the region (N.M. Lemon, pers. comm.). The carbonate platform has a significantly greater carbonate content (approximately 60-80%) probably due to a decreased quartz content compared to the canyon fill. The carbonate again shows evidence of recrystallization to microsparite (10 - 50 μm) and sparry calcite (> 50 μm); the latter is quite abundant up section (Plate 4). The abundant microsparite and sparry calcite stains mauve in alizarin red and potassium ferricynide, and therefore is ferroan.

There is an increase in dolomite content up sequence culminating at the top of the platform with a dolomitized layer just beneath the Bonney Sandstone. The increasing dolomite content is probably due to an increase in shallow water diagenesis. The dolomite of the carbonate platform was possibly formed by early dolomitization of a limestone precursor in a fresh water mixing or supratidal diagenetic zone.

The carbonate of much of the Wonoka Formation canyon and and carbonate platform probably represents a primary marine precipitate. This primary precipitate was probably aragonite a fact suggested by the remnant high strontium concentrations. The aragonite of much of the Wonoka Formation was probably a inorganic precipitate derived from the continental shelf as whitings which were deposited on the shelf and swept down the canyons by turbidity currents and mass flow mechanisms (Figure 22).

Diagenesis of carbonate rocks is anything that occurs from the time of deposition to the onset of metamorphism. Several generations of cementation and compaction of the sediment due to weight of the overlying strata are two of the most prominent of diagenetic change. Diagenesis may include neomorphic change from unstable to stable mineralogy (eg aragonite to low Mg-calcite) and a change in geochemistry. Therefore as sediments are buried and exposed to various different diagenetic environment they come to equilibrium with that environment.

The Wonoka Formation is a shallowing upward sequence and therefore a typical shallowing upward diagenetic sequence should be observed. However, early seafloor cements such as fibrous acicular aragonite coating detrital grains, and later forming void filling mosaic equant spar, was not observed. Instead equant mosaic burial spar forms most of the Wonoka Formation carbonate. This is due to the subsequent burial and recrystallization of the carbonate into ferroan burial spar. Therefore, although these early phases were typically aragonite and high Mg calcite in the late Proterozoic (Tucker 1992), burial diagenesis has transformed it into ferroan calcite.

Plate 3

Canyon Samples Petrography

Plate 3.1:

White light photomicrograph of fine grain micritic and late burial stage ferroan carbonate cement of a silty limestone from Pichi Richi South canyon. Note the late stage cross cutting vein and styolite. (Sample No.: 975-054, Magnification x 10, White light, Exposure=3/100 sec)

Plate 3.2:

Cathodoluminescence photomicrograph of the above sample (Plate 5.1). Note low luminescence of micritic carbonate surrounded and interspersed with high luminescent late stage burial microspar and spar of the cross cutting vein. Dark band to bottom of the photo pressure dissolution stylolite.(Sample 975-054, Magnification x 10, Cathodoluminescence, KV= 19.8 uA=204, Exposure= 3.75 s.)

Plate 3.3:

White light photomicrograph of upper canyon sequence. Dirty very fine grain micrite interspersed with light coloured equant burial microspar. Burial cement has high percentage triple point boundary contacts. (Sample No.: 975-062, Magnification x 20, White light, Exposure= 37 sec)

Plate 3.4:

Photomicrograph of above sample. Note low luminescent micritic carbonate surrounded by high luminescent microspar.Some minor zoning in the later burial spar. Fine grain siliciclastics show bright green and blue luminescence. (Sample 975-062, Magnification x 20, Cathodoluminescence, KV= 19.8, uA=203, Exposure= 3.62 s.)

Chaptern 6: Depositional Model and Discussion of the Wonoka Formation

The nature and origin of the Wonoka Formation canyons is a controversial issue. In this study, however, a submarine model for canyon formation is supported. The finely laminated fine grained sandstones and limestones with interbedded shale which characterises the bulk of the canyon fill represent periods of hemipelagic deposition truncated by turbidites. This sedimentological association, and the classic Bouma sequence observed in the lower canyon fill are cited as compelling evidence for a deep water origin for the Wonoka Formation canyons (Plate 1.6).

The massively bedded sandstones in the basal canyon fill are the highest energy units of the canyon sequence and imply the existence of high velocity proximal turbidity currents. The intraformational conglomerates and the olistostrome units of the canyons were probably derived from mass flow and slumping of the canyon walls during canyon incision and/or canyon filling. Unusual bedding relationships between the main canyon fill and blocks of conglomerate on the sides of many canyons probably can be attributed to these processes.

As suggested by previous authors (Haines,1987, von der Borch et al., 1982) the incision of the canyons probably occurred sometime during deposition of unit 3. This accords with the absence of the lower units in the field area. A deep marine origin for the canyon unconformity is supported by the fact that the overlying and underlying units of both the platform sequence and the canyons are believed to be of deep water facies. Canyon incision probably occurred during a low stand in sealevel when a majority of the sediment load was directly deposited on the shelf slope and proximal turbidity currents eroded the underlying strata.

The canyons were filled by coastal onlap and therefore the sediment fill grades vertically upward into finer grained more shale rich lithologies. The stratigraphic progression from the green silts and sands to the multicoloured fine limestones and siltstones is evidence for this. Infilling was rapid and was probably largely completed by early unit 5. This is supported by the presence of unit 5 in the basal platform sequence and similarities between the basal platform sequence (transitional unit) and the multicoloured canyon fill unit.

Aspects of the geochemistry of the Wonoka Formation canyon fill supports a deep marine origin. The high remnant strontium content of the canyon fill is indicative of an aragonitic mud precursor which has only undergone deep marine diagenesis. Any meteoric influence, which would be pronounced in the event of subaerial exposure would not preserve such high strontium concentrations and values around 200 ppm would be more likely (Scoffin 1887).

Eickoff et al. (1988) suggested that the primary isotopic composition of the Wonoka Formation wallplaster represented the influence of meteoric waters and therefore was strong evidence for subaerial canyon incision. However, the consistency of the isotopic composition for both carbon and oxygen from all the canyon elements (wallplaster, calcareous sandstones, fine grained limestones and intraformational conglomerate clast and matrix) renders this explanation unlikely.

As suggested by Haines (1987), units 5 to 7 represent deposition of a storm dominated, shallowing upward, platform sequence. This interpretation is supported by the present study, and a shoaling upward carbonate platform is suggested for the Devils Peak sequence (Figure 22). The lower carbonate platform sequence of Devils Peak is dominated by sandy event beds cyclically interbedded with shale. Limestone is more abundant in the upper part of the sequence culminating in the supratidal dolomite at the top (Figure 22).

The abundant intraformational conglomerates throughout the sequence are the result of early seafloor cementation and hardgrounds formation. This early seafloor diagenesis or cementation whilst still in the marine phreatic zone is probably due to supersaturation of carbonate in the Proterozoic seas. This suggests that most of the diagenesis of the Wonoka Formation sediments may have largely been complete before any significant burial occured. Therefore the isotopic composition of the Wonoka Formation carbonate platform sequence would have a high probability of retaining a primary isotopic trend.

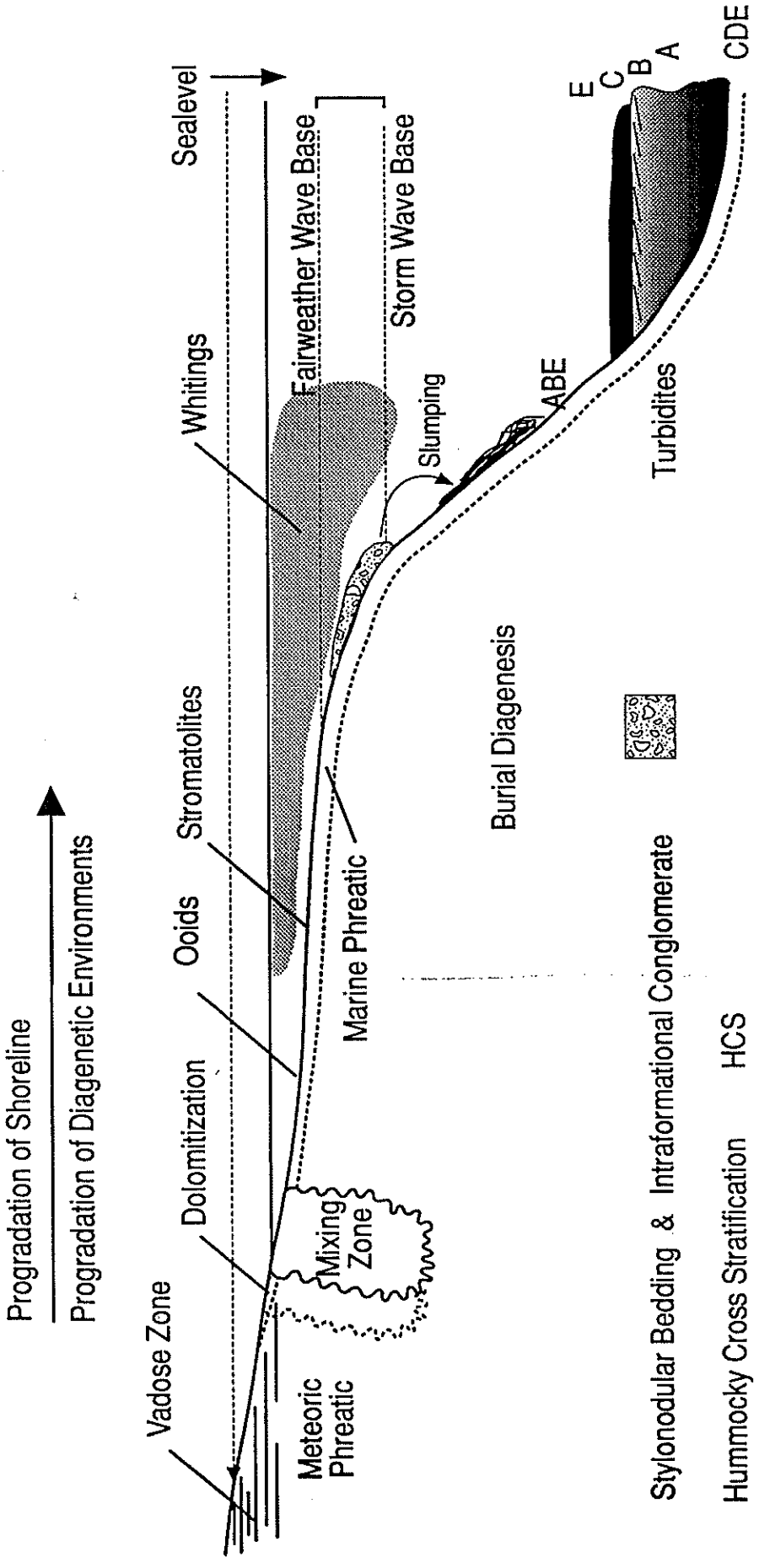

Figure 22: Depositional and diagenetic model for Wonoka Formation platform sequence (after N. Lemon pers. comm.)

Chapter 7: Conclusion

A detailed geochemical stable isotopic and sedimentological study of the late Proterozoic Wonoka Formation has led to the following conclusions:

1) A submarine mechanism is proposed as the preferred model for canyon incision. This is based on the recognition of the Wonoka Formation canyon fill as a deep water sedimentary sequence. Geochemical data from the Wonoka Formation canyons corresponds with the proposed model for the isotopic signal.

2) Strontium isotopic composition for the Wonoka Formation corresponds closely to other established and published isotopic data for the late Proterozoic and therefore a primary strontium isotopic composition is implied.

3) Carbon isotopic composition of the Wonoka Formation remains problematic. Highly consistent isotopic trends across the basin support a primary origin for the carbon isotope values. However, until recently there has been an absence of similar published isotopic trends for late Proterozoic strata and only with further work will the validity of the model for such highly negative carbon isotope data be established.

4) An aragonitic precursor for the primary marine carbonate precipitate in the late Proterozoic is supported by the remnant high strontium concentrations of the Wonoka Formation.

5) Geochemical evidence suggests that the Wonoka Formation canyon sequence was exposed to only submarine and late stage burial diagenesis to ferroan microsparite and sparry calcite.

6) Geochemical petrographic and sedimentological evidence supports a shallowing upward succession for the Wonoka Formation formation carbonate platform sequence culminating in superatidal or mixing zone dolomitizatiion of the uppermost Wonoka Formation of the southern Flinders Ranges.

Acknowledgements

There are numerous people I would like to thank for their help during such a demanding but worthwhile year.

Firstly I would first like to thank those intimately associated with my work and topic David McKirdy, Richard Jenkins and Ben Urlwin who always kept me thinking and working when I came up with some crazy ideas. I would especially would like to thank Ben for his effort and companionship during our sometimes insane but entertaining field trip to the Flinders Ranges. I would also like to thank Nick Lemon and Martin Kennedy for the help during the year and in refining my thesis.

To all the technical staff especially Keith, Wayne, Jeff, ,Phill, Michelle and Hue who without it would have been impossible to compile such a thesis. To the office staff Sherry, Sophie and Bronwyn who helped with messages and frantic questions about thesis preparation and drafting.

I would like to thank the Department of Geology for the use of a departmental vehicle during my mapping exercise in August .

To almost all of the property owners in my field areas who allowed me access to their properties and to Mr and Mrs Drennan at the Pichi Richi Holiday Camp for their kind hospitality during my field work. A special thanks to Rob and Di at the Transcontinental Hotel for a couple of nights accommodation and a few cold beers.

I would like to thank all the other honours students for putting up with my silly antics and for an entertaining but enjoyable year. To a few of my good friends from Lincoln Pove Sladey Mick and Tash and the numerous friends from last year John, Scotty, Bruce and the rest of the mob who I could not catch up with as much as I would have liked .

Last but certaintly not least I would like to thank Kirrilie and her family and my parents and brothers Mick and Kym who all played an important part in helping me through my **LAST** year of uni.

References

Aharon, P., Schidlowski, M. & Singh, I. B., 1986. Chronostratigraphic markers in the end-Precambrian carbon isotope record of the Lesser Himalaya. *Nature* 327: 699-703.

Anderson, T.F. & Arthur, M.A., 1983. Stable isotopes of oxygen and carbon and their application to sedimentological and palaeoenvironmental problems. In *Stable isotopes in sedimentary geology.* SEPM (Society of Economic Palaeontologists and Mineralogists) Short Course 10: 1-151.

Asmerom, Y., Jacobsen, S.B., Knoll, A.H., Butterfield, N.J. & Swett, K., 1991. Strontium isotopic variations of Neoproterozoic seawater: Implications for crustal evolution. *Geochimica et Cosmochimica Acta* 55: 2883-2894.

Brand, U., & Veizer, J., 1980. Chemical Diagenesis of a multicomponent carbonate system-1: Trace Elements. *Journal of Sedimentary Petrology* 50: 1219-1236.

Brand, U., & Veizer, J., 1981. Chemical Diagenesis of a multicomponent carbonate system-2: Stable Isotopes. *Journal of Sedimentary Petrology* 51: 987-997.

Brasier, M.D., 1992. Global ocean-atmosphere change across the Precambrian-Cambrian transition. *Geological Magazine* 129 (2): 161-168

Brasier, M.D., Magaritz, M., Corfield, R., Huilin, L., Xiche, W., Lin, O., Zhiwen, J., Hamdi, B., Tinggui, H. & Fraser, A.G., 1990. The carbon and oxygen-isotope record of the Precambrian-Cambrian boundary interval in China and Iran and their correlation. *Geological Magazine* 4: 319-332.

Brasier, M.D., Anderson, M.M. and Cornfield R.M., 1992.Oxygen and carbon isotope stratigraphy of early cambrian carbonates in southeastern Newfoundland and England. *Geological Magazine* 129 (3): 265-279.

Christie-Blick, N. von der Borch, C.C., and DiBona, P.A., 1990 Working Hypothesis for the orgin for the origin of the Wonoka canyons (neoproterozoic), South Australia. *American Journal of Science* 290-A: 295-332.

Cloud and Glassener 1982.The Ediacarian Period and system: Metozoans inhert the Earth. *Science* 217: 783-792.

Coats R.P. 1964. Large scale Precambrian slump structure structure, Flinders Ranges. Quarterly Geological Notes, Geological Survey South Australia. 11: 1-2.

Coats, R.P., 1973. Copely, South Australia . Explanantory notes, 1: 250 000, Geological Series. Sheet SH/ 54-9, Geological Survey of South Australia.

Dalgarno, C.R. and Jonhson, J.E., 1964. The Wilpena Group. IN Thompson et al., Precambrian rock groups in the Adelaide Geosyncline: a new subdivision. Quartly Geological Notes, Geological Survey of South Australia, 9: 7-12

Degens, E.T., 1971. Stable isotope distrbution in carbonates In Chilingar G.V., Bissell, H.J. and Fairchild, R.W. eds, *Carbonate rocks: Developments in Sedimentology* 9B: 193-208.

Derry, L.A., Keto,L.S., Jacobsen, S.B., Knoll, N.J. & Swett, K., 1989. Sr isotopic variations in Upper Proterozoic carbonates from Svalbard and East Greenland. *Geochimica et Cosmochimica Acta* 53: 2331-2339.

Derry, L.A.,Kaufman A.J., & Jacobsen, S.B.,1992. Sedimentary cycling and environmental change from stable and radiogenic isotopes *Geochimica et Cosmochimica* Acta 56: 1317-1329.

DiBona, P.A., von der Borch, C.C. & Christie-Blick, N.,1990. Sequence stratigraphy and evolution of a basin-slope succession: The Late Proterozoic Wonoka Formation , Flinders Ranges, South Australia. *Australian Journal of Earth Science* 37: 135-145.

Eickoff, K. H., von der Borch, C.C., and Grady, A.E., 1988. Proterozoic canyons of the Flinders Ranges (South Australia): submarine canyons or drowned rivers. *Sedimentary Geology* 58: 217-235.

Fairchild, I.J. and Spiro, B., 1987. Petrological and isotopic implications of some contrasting Late Precambrian carbonates, NE Spitsbergen. *Sedimentology* 34: 973-989.

Fairchild, I.J., Marshall, J.D. & Bertrand-Sarfati, J., 1990. Stratigraphic shifts in carbon isotopes from Proterozoic stromatolitic carbonates (Mauritania): Influences of primary minerology and diagenesis. *American Journal of Science* 290-A: 46-79.

Friedman, G.M. and Sanders, J. E., 1974. Positive-relief bedforms on modern tidal flat the resemble molds of flute and grooves;implications for geopetal criteria and for origin and classification of bedforms. *Journal of Sedimentary Petrology* 44: 181-189.

Faure, G., 1986. *Principals of Isotope Geology 2nd edition.* John Wiley & Sons.

Gostin, V.A. & Jenkins, R.J.F. 1983. Sedimentation of the early Edicacaran, Flinders Ranges, South Australia. *Geological Society of Australia Abstracts* 9: 196-197.

Gostin, V.A., Haines , P.W., Jenkins, R.J.F., Compston W. & Williams, I.S. 1986. Impact ejecta horizon within late Precambrian shales, Adelaide Geosyncline. Science 233: 198-200.

Haines, P.W. 1986., Late Precambrian carbonate shelf to shale basin transition Wonoka Formation, Flinders Ranges, South Australia. *Geological Society of Australia Abstracts* 15: 92-93.

Haines, P.W., 1987. Carbonate shelf and basin sedimentation, late Proterozoic Wonoka Formation, South Australia. PhD Thesis, University of Adelaide (unpubl.).

Haines, P.W.,1988. Storm-dominated mixed carbonate/ siliciclastic shelf sequence displaying cycles of hummocky cross-stratification, late Proterozoic Wonoka Formation, South Australia. *Sedimentary Geology* 58: 237-254.

Haines, P.W., 1990. A late Proterozoic storm-dominated carbonate shelf sequence: The Wonoka Formation in central and sourthern Flinders Ranges, South Australia. In Jago J.B. & Moore P.S. : The evolution of a late Precambrian-Early Palaeozoic rift complex: The Adelaide Geosyncline. *Geological Society of Australia Special Publication* 16: 179-194.

Hudson, J. D., 1977. Stable isotopes and limestone lithification. *Quarterly Journal of the Geological Society London.* 133: 637-660.

Hudson, J. D., 1975 Carbon isotopes and limestone cement. *Geology* January: 19-22

Irwin H. & Curtis C., 1977. Isotopic evidence for source of diagenetic carbonate formed during burial of organic-rich sediments. Nature 269: 209-213.

Jansyn, J., 1990. Strato-tectonic evolution of alarge subsidence structure associated with the late Proterozoic Wonoka Formation at Wilpena Pound, central Flinders Ranges, South Australia. B.Sc. Honours Thesis, University of Adelaide (unpubl.).

Jenkins R.J.F., 1990. The Adelaide Fold Belt: Tectonic reapprasial. In Jago J.B. & Moore P.S. : The evolution of a late Precambrian-Early Palaeozoic rift complex: The Adelaide Geosyncline. *Geological Society of Australia Special Publication* 16: 396-420.

Jenkins R.J.F. 1981. The concept of an "Ediacaran Period" and its stratigraphic significance in Australia. *Transactions of the Royal Society of Austalia* 105: 177-194.

Jenkns, R.J.F. & Gostin, V.A., 1983. Marinoan and Ediacarian type sections in the context of tectonic cycles in the Adelaide Geosyncline. Geological Society of Australia Abstracts 10: 39-44.

Jenkins, R.J.F., McKirdy, D.M., Foster,C.B., O'Leary, T. & Pell S.D., 1992. The record and stratigraphic implications of organic-walled microfossils from the Ediacaran (terminal Proterozoic) of South Australia. *Geological Magazine* (in press).

Kaufman, A.J., Hayes J.M., Knoll, A.H. & Germs G.J.B., 1991. Isotopic compositions of carbonates and organic carbon from upper Proterozoic successions in Namibia: stratigraphic variation and the effects of diagenesis and metamorphism. *Precambrian Research.* 49: 301-327.

Kaufman, A.J., Knoll, A.H. & Awranik, S.M., 1992. Biostratigraphic and chronostratigraphic correlation of Neoproterozoic sedimentary successions: Upper Tindir Group, north western Canada, as a test case. Geology 20: 181-185.

Knoll, A.H., Hayes, J.M., Kaufman, A.J., Swett, K. & Lambert, I.B., 1986. Secular variations in carbon isotope ratios from Upper Proterozoic successions of Svalbard and east Greenland. *Nature* 321: 832-838.

Knoll, A.H., 1991. End of the Proterozoic Eon. *Scientific American* Oct.: 42-49.

Knoll A.H. & Walter M.R., 1992. Latest Proterozoic stratigraphy and earths history. *Nature* 356: 673-678.

Lambert, I.B. & Donnelly, T.H., 1991. Atmospheric oxygen levels in the Precambrian a review of isotopic and geological evidence. Palaeogeography, Palaeochlimatology, Palaeoecology 97: 83-91.

Lambert, I.B., Walter, M.R., Wenlong, Z., Sangnian, L. & Guogan, M., 1987. Palaeoenvironmental and carbon isotope stratigraphy of Upper Proterozoic carbonates of the Yangtze Platform: *Nature* 325: 140-142.

Latham, A. & Riding, R., 1990. Fossil evidence for the location of the Precambrian/Cambrian boundary in Morocco: *Nature* 344: 752-754

McNoughton, N.J. and Withnall, I.W. 1985. Carbonate ^{13}C and 18O depletion during regional metamorphism. In Herbet, H.K. and Ho, S.E. eds. 1990. *Stable Isotopes and Fluid Processes in Mineralization.* Publication No. 23, Geology Department and University Espension, University of Western Australia.

Magaritz, M., Holser, W.T. & Kirschvink, J.L., 1986. Carbon-isotope events across the Precambrian/Cambrian boundary on the Siberian Platform. *Nature* 320: 258-259.

Magaritz, M., Bar, R., Baud, A. & Holser, W.T., 1988. The carbon-isotope shift at the Permian/Triassic boundary in the southern Alps is gradual. *Nature* 331: 337-339.

Magaritz, M., 1989, 13C minima follow extinction events: a clue to faunal radiation: *Geology* 17: 337-340.

Magaritz, M., 1990 Carbon isotopes, time boundaries and evolution. *Terra Nova* 3: 251-256.

Magaritz, M., Benjamini, C., Keller, G. & Moshkovitz, S., 1992. Early diagenetic isotopic signal at the Cretaceous/Tertiary boundary, Israel. *Palaeogeography, Palaeoclimatology, Palaeoecology* 91: 291-304.

Marshall, J.D., 1992. Climatic and oceanographic isotopic signals from the carbonate rock record and their preservation. *Geological Magazine* 129 (2): 143-160.

Pell, S., 1989. Stable isotope composition of organic matter and coexisting carbonate in the late Precambrian of the Officer Basin. Stratigraphic relationships with neighbouring basins and enviromental significance. B.Sc.Honours Thesis, University Of Adelaide (unpubl.).

Plummer, P.S., 1978. Stratigraphy of the lower Wilpena Group (late Precambrian),Flinders Ranges, South Australia. *Transactions of the Royal Society of South Australia.* 102: 25-38.

Preiss, W.V., 1987. The Adelaide Geosyncline - late Proterozoic stratigraphy, sedimentation, palaeotology and tectonics. *Geological Survey of South Australia Bulletin* 53.

Preiss, W.V., 1990. A stratigraphic and tectonic overview of the Adelaide Geosyncline, South Australia. In Jago J.B. & Moore P.S. : The evolution of a late Precambrian-Early Palaeozoic rift complex: The Adelaide Geosyncline. *Geological Society of Australia Special Publication* 16: 1-33.

Royse, C.F. Jr.,Wardell, J.S., Peterson, L.E. 1971. X-ray determination of dolomite-calcite : an evaluation. *Jouranal of Sedimentary Petrology.* 41: 483-488.

Schidlowski, M., 1988. A 3800-million-year isotopic record of life from carbon in sedimentary rocks. *Nature* 333: 313- 318.

Scoffin, T.P. (1987) *An introduction to Carbonate sediments and rocks.* Blackie & Sons Limited. Glasgow.

Singh, U., 1986 Late Precambrian and Cambrian carbonates of the Adelaidean in the Flinders Ranges, South Australia- A petrographic, electron microprobe and stable isotope study. PhD Thesis: University of Adelaide (unpubl.).

Sukanta, U., Thomas, B., von der Borch, C.C. & Gatehouse, C.G., 1991. Sequence stratigraphic studies and canyon formation, South Australia. PESA Journal. Sept.: 68-73.

Thompson, B.P., Mirams, R.C., Forbes, B.C., Dalgarno, C.R. & Johnston, J.E., 1964. Precambrian rock groups in the Adelaide Geosyncline: a subdivision. Quarterly Geological Notes, Geological Survey of South Australia 9: 1-10

Tucker, M.E., 1990. Carbon isotopes and Precambrian-Cambrian boundary geology, South Australia: ocean basin formation, sea water chemistry and organic evolution. *Terra Nova* 3: 573-582.

Tucker, M.E., 1992. The Precambrian - Cambrian boundary: seawater chemistry, ocean circulation and nutrient supply in metazoan evolution, extiction and biomineralization. *Journal of the Geological Society London.* 149: 655-688

Tucker, M.E., and Wright, V.P. 1990. *Carbonate Sedimentology* Blackwell Scientific Publications Oxford.

Urlwin, B., 1992. Carbon Isotope Stratigraphy of the late Proterozoic Wonoka Formation of the Adelaide Fold Belt: Diagenetic Assessment and Interperation of Isotopic Signature and Correlation with previously measured isotopic curves. BSc. Honours Thesis Universiy of Adelaide (unpubl.).

von der Borch, C.C., Smit, R., and Grady, A.E., 1982. Late Proterozoic submarine canyon, Adelaide Geosyncline, South Australia. *The American Association of Petroleum Geologists Bulletin* 66,3: 332-347.

von der Borch, C.C. and Grady, A.E., 1984. Mechanisms of sandstone deposition in a late Proterozoic submarine canyon, Adelaide Geosyncline, South Australia. *The American Association of Petroleum Geologists Bulletin* 68: 684-689.

von der Borch, C.C., Grady, A.E., Aldam, R., Miller, D. Neumann, R., Rovira, A., and Eickoff, K., 1985. A large-scale meandering submarine canyon: outcrop example from the late Proterozoic Adelaide Geosyncline, South Australia. Sedimentology 32, 507-518.

von der Borch, C.C., Christie-Blick, N. & Grady, A.E., 1988. Depositional sequence analysis applied to Late Proterozoic Wilpena Group, Adelaide Geosyncline, South Australia. *Australian Journal of Earth Sciences* 35: 59-71.

von der Borch, C.C., Grady, A.E., Eickoff, K.H., DiBona, P.A., and Christie-Blick, N., 1989. Late Proterozoic Patsy Spring Canyon, Adelaide Geosyncline: submarine or subaerial origin? *Sedimentology* 36: 777-792.

Wallace, M.W., Gostin, V.A. & Keays, R.R., 1989. Acraman Impact ejecta blanket in the Officer Basin. *Australian Journal of Earth Science* 36: 585-587.

Williams, G.E., 1986. The Acraman Impact Structure. Source of ejecta in the late Precambrian shales. *Science* 233: 200-202.

Veizer, J., 1983. Chemical diagenesis of carbonates: Theory application of trace element technique. In *Stable isotopes in Sedimentary Geology* (ed M.A. Arthur et al.) Society of Palaeontologists and Mineralogists, Short Course No. 10,

Appendix 1 Analytical Methods

Analytical procedures and techniques used were:

1) Rock Surface Staining and Etching
2) Acetate Peels
3) Thin Secton Petrography including:
   Optical & Cathodoluminescence microscopy.
4) Organic and Inorganic Carbon Estimation by Loss on Ignition
5) X-Ray Diffraction
6) Stable Carbon and Oxygen Isotope Analysis
7) Atomic Absorption Spectrometry
8) Strontium Isotope Analysis

Sample etching and staining.

Samples etched and stained:

Rock samples that were slabed and polished for peel application.
Half thin sections for optical microscopy.

Samples were etched and stained using a procedure and solutions adapted from Dickson (1965).

Solutions:

Alizarin Red Solution	Potassium Ferricyanide Solution
- O.2 g Alizarin Red S	- 2.0 Potassiun Ferricyanide
-100 mls 1.5M HCL	- 100 mls 1.5M HCL

Procedure for sample and slide etching and staining:

1. Etch for 15 seconds in 1.5M HCL.
2. Wash quickly with distilled water.
3. Stain for 45 seconds in 3:2 ratio of alizarin red and potassium ferricyanide solution.
4. Wash quickly with distilled water.
5. Stained for 15 sconds in Alizarin Red Solution.
6. Wash quickly with distilled water.
7. Allow sample to dry.

Stained Acetate Peels

Acetate peels were made using a proceedure adapted from Tucker (1988)and solutions as above from Dickson (1965).

Procedure

1) Selected samples were slabed and polished to remove any saw cuts on the surface.
2) Samples were stained using the above 'Sample etching and staining procedure'.
3) Dried stained slabs and acetate were refrigerated.
4) Sample was leveled in a covered sand tray.
5) A small pool of acetate was flooded onto one end of the stained rock surface.
6) Acetate film was applied by rolling across rock surface to squeeze out any excess acetate.
7) Dry Acetate Peel removed and examined

Thin Secton Petrography

Optical Microscopy

1) Thin sections made by departmental lapidary were analysed under normal and polarised light for minerological and petrographic composition

Cathodoluminescence Microscopy

1) Thin sections were analysed under cathodoiluminescence to determine phases of carbonate precipitation (ie. primary or secondary carbonate).

Cathodoluminescence Conditions
Approxmately 20 kV and 200 mA.

Organic and Inorganic Carbon Estimation by Loss on Ignition

Procedure

1) Three to four grams of powdered sample was placed in a oven at 110 °C overnight to remove any surface moisture.
2) Powdered sample was removed from oven and placed in a desicator to cool to room temperature.
3) Using Sartorious Electronic Balance and Sedloss Computer Program each of the alumina crucibles were weighed and logged.
4) A cool dried powdered sample was added to each crucible and Crucible+Sample weight logged.
5) The crucibles were then placed in a silica tray and ignited at 500°C in the muffel furnace for one hour.
6) After one hour the ignited samples were removed from the furnace and cooled to room temperature in a desicator.
7) The crucible+sample was then weighed and logged and the samples loss on ignition at 500°C or organic carbon estimate calculated.
8) The samples were then returned to the muffel furnace and ignited at 1000°C for one hour.
9) Cooled samples were weighed and the samples loss on ignition at 1000°C or carbonate carbon estimate calculated.

X-Ray Diffraction

X-Ray diffraction was performed on samples to find constituent mineral phases particularly carbonate phase and calcite to dolomite contemt

Sample Preperation

1) Powdered rock sample was ground into an equidimensional grain size using a pestel and motar.
2) To motar was added three to four drops of water and fine powder mixed into a smooth paste.
3) The paste was then smeared evenly across a glass XRD slide with identification number attached to one end.
4) Slide was the allowed to dry for a couple of days or in an oven at 115°C.

X-Ray Diffraction cont.

Sample Analyses

5) The sample was then analysed using Siemens X-Ray Diffractometer using a cobalt tube set at a scan speed of 1° per minute.
6) The samples resultant XRD diffractograms were analysed for mineralogical composition using JCPDS computer file.
7) Percentage calcite and dolomite was calculated and, their purity and cation composition calculated using computer programs and correction curves.

Stable Carbon and Oxygen Isotope Analysis

Sample Preperation

1) Samples Selected for carbon and oxygen isotope analysis were drilled with dentist drill carefully selecting areas unweathered or without calcite veins.
2) Approxmately 15-25 mg of sample was weighed using Saugtorsis Electronic Balance and placed in one arm of a reaction tube.
3) 4 mls of 100% H2PO3 (phosphoric acid) added to other arm of reaction tube
4) Evacuate reaction tube using isotope line.
5) Sample equilibrated and reacted:

    1. Carbonate reacted at 25 C for 10 - 16 hours.

    2. Mixed Dolomite / Calcite samples
       Calcite fraction reacted at 25 C for 30min.
       Dolomite fraction reacted at 50 C for 10 -16 hours.

6) Samples collected after reaction time on isotope line.

Sample Analyses

7) Samples analysed for carbon and oxygen iosotopes on Isogas mass spectrometer realitive to PDB standard.

Major and Trace Metal Analyses via Atomic Absorption

Sample dissolution

1) Teflon beakers were washed in 5 M Nitric Acid and rinced 3 times with deionized water.
2) 1g of powdered rock sample was weighed into teflon beaker.
3) To each beaker a small amount of deionized water and 20 mls of acetic acid was added.
4) The teflon beakers were warmed gently to dissolve carbonate fraction and evaporate the acetic acid.
5) Samples acetate crystals were redissolved in 10mls acetic acid and filtered using 54 hardened filter paper into 100ml volumetric flask.
6) 10mls of potassium and lathaum solution (La/K) was added and volumetric flask made up to volume using deionized water.
7) 20 times dilution of solution was made by adding:
   5 mls of sample concentrate solution, 9.5 mls acetic acid, 9.5 mls La/K solution to 100ml Volumetric Flask Make and making flask up to volume with deionized water.

Sample Analyses

Samples were analysed using Varian AA-S atomic absorbtion spectrometer for selected trace and major elememts Sr, Rb, Fe, Mg, Mn, and Ca in an air acetelyene flame. Major and trace element concentraction were calculated in parts per million as in Appendix 2

Strontium Isotopic Analysis

Samples were selected for strontium isotope analysis on the following critera as outlined by Derry et al 1989, 1992 and Asmerom 1991: low Mn /Sr, no rubidium, no dolomite (< 10%). Strontium isotope analysis was performed as follows:

1) Approxmately 100 milligrams of drilled samples was reacted in a clean teflon beaker with 8 mls of 1N HCL for 1 hour.
2) Dissolved sample was pipetted off carefully avoiding any non dissolved solid residue.
3) Pipetted solution was placed in clean centrifuge tube and centrifuged for 10 minutes at 3000rpms.

Strontium Isotopic Analysis cont.

4) Clear solution was pipeted off avoiding solid residue and placed in another clean centrifuge tube and centrifuged for 10 minutes at 3000rpms
5) Final solution was pipetted off and placed in a clean teflon beaker and evaporated dry on a teflon coated hot plate at 200°C
6) Solid fraction was redissolved in 1.5 ml of 3N HCL and ran through two stage cation exchange columbs where strontium collected for isotopic composition analysis.
7)The strontium solution was evaporated to dryness on hotplate.

Sample Analysis

8) The strontium solid fraction was redissolved in 1µL of H3PO4 and mounted on single titanium filamaent and evapourated dry.
9) Samples were loaded on filimant magazine and run on Finnigan MAT261 mass spectrometer analysing strontium 87 / 86 ratio.

Appendix 2 Geochemical Data

Stable Carbon and Oxygen Isotope Data
Loss on Ignition
XRD MIneralogy
Major and Trace element Atomic Absorption
Trace Element Ratios
Strontium Isotopic Data

TABLE YIELD +ISO

SAMPLE NO.	METRES	% YIELD	∂ 13C	∂ 18O
975-001	0.0	30.50	-7.799	-14.126
975-010	38.0	52.80	-8.020	-13.616
975-019	79.8	37.20	-7.923	-13.952
975-026	123.4	47.59	-7.639	-13.999
975-033	147.9	32.30	-7.551	-13.746
975-038	185.5	60.80	-7.529	-13.010
975-046	215.5	36.80	-7.483	-13.254
975-054	221.5	63.20	-7.355	-13.060
975-062	276.8	63.40	-7.901	-13.243
975-067	350.7	41.59	-7.763	-13.506
975-070 DOL	368.0	23.77	-0.886	-10.835
975-070 CAL	368.0	31.48	-1.817	-8.206
975-071 DOL	264.0	12.70	-1.371	-10.447
975-071 CAL	264.0	11.35	-0.810	-7.506
975-075	249.5	83.99	-1.116	-12.555
975-080	331.1	78.03	-1.173	-12.125
975-086M	306.0	56.75	-2.504	-11.393
975-086C	306.0	75.58	-2.493	-11.556
975-087C	202.0	76.85	-3.907	-10.890
975-089	178.0	79.77	-3.872	-12.023
975-098	162.0	50.26	-4.187	-11.023
975-104	147.4	69.60	-5.803	-12.729
975-111	107.8	23.12	-7.448	-14.105
975-115	55.1	51.20	-7.345	-13.258
975-202	16.7	35.80	-7.980	-14.238
975-209	134.5	38.44	-8.027	-13.925
975-221	246.8	60.32	-7.368	-13.501
975-301	341.0	56.41	-7.446	-13.091
975-311	0.0	30.69	-8.414	-15.140
975-317	172.0	46.40	-7.769	-14.435
975-322	258.1	73.40	-8.895	-17.141
975-324	340.0	74.35	-7.887	-14.711
975-402	-	82.68	-8.570	-15.264
975-406	-	1.70	-6.937	-12.590
975-407C	-	57.70	-8.894	-15.289
975-407M	-	87.84	-8.330	-15.078
PRS CV	-	99.00	-7.284	-13.899
DPS CV	-	84.00	-7.684	-13.524
ANU-PRM2	-	90.00	0.745	-17.289
ANU-PRM2	-	92.54	0.683	-17.633
ANU -P3	-	98.14	2.231	-0.573

Loss on Ignition Table

Sample No.	% Loss on Ignition @ 500 °C	% Loss on Ignition @ 1000 °C	Total % Loss on Ignition
975-001	0.848	15.393	16.241
975-010	0.971	25.309	26.280
975-019	1.059	17.929	18.988
975-026	0.887	21.926	22.813
975-033	0.774	30.773	31.547
975-038	1.012	29.977	30.989
975-046	0.495	19.937	20.432
975-054	0.614	29.639	30.253
975-062	0.771	23.548	24.319
975-067	0.699	20.608	21.307
975-070	0.712	29.751	30.463
975-071	0.725	13.688	14.413
975-075	0.438	37.772	38.210
975-080	0.424	24.949	25.373
975-086	0.303	35.711	36.014
975-089	0.361	35.569	35.930
975-098	0.546	39.151	39.697
975-104	0.577	33.894	34.471
975-111	0.886	13.755	14.641
975-115	0.680	25.898	26.578
975-202	0.572	19.121	19.693
975-209	0.421	17.058	17.479
975-221	0.193	29.870	30.063
975-301	0.324	28.965	29.289
975-311	0.265	15.525	15.790
975-317	0.211	25.520	25.731
975-322	0.384	35.409	35.793
975-324	0.603	33.753	34.356
975-366	0.242	14.146	14.388
975-402	0.341	36.198	36.198
975-406	0.443	3.981	4.424

XRD mineralogy

Sample No.	% D = D/D+C	% Quartz	% Calcite	% Dolomite	% Albite	% Muscovite	% Chlorite
975-001		42.0	34.0		12.0	5.0	5.0
975-010	4.2	24.0	55.0	2.5	7.0	5.0	5.0
975-019	7.6	38.9	36.8	2.8	9.5	6.4	5.4
975-026		31.4	50.7		6.6	5.4	5.2
975-033		15.8	68.5		5.8	5.1	4.5
975-038		21.8	63.4		5.4	4.8	4.4
975-046		38.7	36.1		11.2	6.4	7.3
975-054		19.1	67.1		4.2	4.9	4.4
975-062		30.1	52.8		6.5	5.0	5.2
975-067		40.5	37.6		12.2	4.2	5.2
975-070	71.2	30.6	14.9	37.0	4.4	6.5	6.3
975-071	42.6	46.5	15.1	11.2	7.2	10.5	9.3
975-075	5.8	22.4	70.4	4.3	2.6		
975-080	7.5	15.4	72.4	5.8	2.5		3.5
975-086	2.2	14.9	79.5	1.8			3.7
975-089	2.3	7.9	84.2	3.1	2.0		2.7
975-098	11.5	34.3	44.7	5.8	6.8	4.1	4.1
975-104		15.1	73.4		4.2	4.2	3.0
975-111	11.0	42.0	28.5	3.5	11.8	7.9	6.1
975-115	6.1	27.6	53.9	3.5	4.4	5.4	4.9
975-366		31.2	46.4		11.3	5.5	5.4
975-202		30.0	46.4		8.1	11.6	8.7
975-221	3.1	17.1	65.2	2.1	4.4	5.3	5.6
975-301		17.2	68.5		5.6	5.6	2.9
975-311	28.3	24.9	42.6	9.8	1.4	5.9	5.0
975-317	6.5	22.4	543.4	3.7	11.4	7.6	6.7
975-322	4.7	8.9	76.7	3.7	6.2	4.3	
975-324		12.3	76.9		5.4	5.2	
975-402		17.6	71.8		5.7	6.2	3.5
975-404		44.4	40.3		8.2	4.9	
975-406		58.2	4.8		10.1	8.9	20.2

Element Appendix

Sample No	Ca (ppm)	Mg (ppm)	Fe (ppm)	Mn (ppm)	Sr (ppm)	Rb (ppm)
975-001	523803.28	9406.56	6360.66	1255.74	980.33	0
975-010	457575.76	7651.52	5492.42	384.47	2757.58	0
975-026	483042.66	4250.89	3824.33	691.32	1311.20	0
975-038	497203.95	7565.79	4835.53	580.59	3546.05	0
975-054	494398.73	4248.42	2500.00	474.68	1610.76	0
975-062	360252.37	3974.76	3091.48	556.78	1968.45	0
975-071	368066.53	120249.48	25114.35	7430.35	257.80	0
975-075	439409.45	10334.56	3809.98	1397.79	326.23	0
975-086	517392.07	6114.54	5145.37	1406.17	909.25	0
975-098	449542.38	20891.36	7560.68	2192.60	957.02	0
975-104	522500.00	6530.17	3821.84	991.38	696.84	0
975-115	494375.00	9687.50	5703.13	994.14	804.69	0
975-221	516379.31	5422.75	3348.81	518.90	1664.46	0
975-301	537706.08	3568.52	2481.83	639.96	1014.00	0
975-311	405017.92	34604.11	19615.51	7546.43	325.84	0
975-317	535387.93	9765.09	5862.07	1049.57	846.98	0
975-322	475013.62	8937.33	3106.27	3430.52	423.71	0
975-402	472472.18	3870.34	1765.84	828.50	596.27	0

Element Ratios

Sample No	Mn/Sr	Ca/Sr	Mg/Ca
975-001	1.281	534.314	0.018
975-026	0.527	368.397	0.009
975-054	0.295	306.935	0.009
975-071	28.823	1427.742	0.327
975-086	1.547	569.031	0.012
975-104	1.423	749.814	0.012
975-221	0.312	310.239	0.011
975-301	0.631	530.280	0.007
975-311	23.160	1243.000	0.085
975-317	1.239	632.112	0.018
975-402	1.389	792.373	0.008
975-010	0.139	165.934	0.017
975-038	0.164	140.213	0.015
975-062	0.283	183.013	0.011
975-075	4.285	1346.934	0.024
975-098	2.291	469.730	0.046
975-115	1.235	614.369	0.020
975-322	8.096	1121.093	0.019

Appendix 3 Petrographic Discriptions

Sample Number: 975-001

Location: Pichi Richi South Canyon

Mineralogy:

Quartz 60%
Calcite 20%
Albite 5%
Muscovite 5%
Chlorite 7%
Other 3%

Description: Very fine grain (10 -50um) angular detrital quartz. Microsparitic ferroan calcite cement. Interbedded quartz and calcite rich and shale rich layers.

Classification: Calcite cemented sandstone

Sample Number: 975-010

Location: Pichi Richi South Canyon

Mineralogy:

Quartz 65%
Calcite 25%
Albite 5%
Muscovite 5%
Chlorite 8%
Other 2%

Description: Very fine grain (10 -50um) angular detrital quartz. Microsparitic ferroan calcite cement. Interbedded quartz/calcite rich and shale rich layers. Basal sand unit

Classification: Calcite cemented sandstone

Sample Number: 975-019

Location: Pichi Richi South Canyon

Mineralogy:

Quartz 65%
Calcite 25%
Albite 4%
Muscovite 8%
Chlorite 8%
Other

Description: Very fine grain (10 -50um) angular detrital quartz. Microsparitic ferroan calcite cement. Interbedded quartz and calcite rich and shale rich layerslaminated mica rich and quartz and calcite rich layers Sedimentary structures crossbedding and graded bedding. Heavey mineral laminations

Classification: Calcite cemented sandstone

Sample Number: 975-026

Location: Pichi Richi South Canyon

Mineralogy:

Quartz 40%
Calcite 40%
Albite 5%
Muscovite 5%
Chlorite 8-10%
Other 2%

Description: Laminated quartz and calcite rich and mica rich layers aligned to shistosity. Very fine grain (10 -50um) angular detrital quartz possibly due to alkaline attack. Equant ferroan calcite cement recrystallized from micrite and microsparite cement.

Classification: Fine grain silty limestone (Calcisiltite)

Sample Number: 975-033

Location: Pichi Richi South Canyon

Mineralogy:

Quartz 20%
Calcite 60%
Albite 5%
Muscovite 5%
Chlorite 4%
Other 5% opaques

Description: Very fine grain quartz (10 50um) angular to sub rounded with quartz overgrowths . Purple or mauve staining ferroan calcite cement and micrite recrystallized microsparite. Calcite cement equent with triple point boundaries. Minor secondary calcite filled veins.

Classification: Fine grain silty limestone microsparite or calcisiltite

Sample Number: 975-038

Location: Pichi Richi South Canyon

Mineralogy:

Quartz 20%
Calcite 60%
Albite 5%
Muscovite 8%
Chlorite 5%
Other 2%

Description: Very fine grain (10 -50um) laminate limestone mixed micrite matrix and microspar cement. Calcite has be recrystallized into equant ferroan microsparite.

Classification: Fine grain silty limestone (microsparite or calcisiltite)

Sample Number: 975-046

Location: Pichi Richi South Canyon

Mineralogy:

Quartz 40%
Calcite 40%
Albite 5%
Muscovite 5%
Chlorite 8-10%
Other 2%

Description: Laminated quartz and calcite rich and mica rich layers. Chlorite alteration of muscovite with some bedding plane orentation of micas. Very fine grain (10 -50um) angular detrital quartz. Ferroan calcite cement and micrite which has been recrystallized to microsparite.

Classification: Fine sandy limestone or calcarous sandstone (calcisiltite,microsparite)

Sample Number: 975-054

Location: Pichi Richi South Canyon

Mineralogy:

Quartz 40%
Calcite 40%
Albite 5%
Muscovite 5%
Chlorite 8-10%
Other 2%

Description: Laminated quartz and calcite rich and mica rich layers. Very fine grain (10 -50um) angular detrital quartzwith overgrowths. Equant ferroan calcite cement recrystallized microsparite.

Classification: Fine grain silty limestone (Calcisiltite or microsparite)

Sample Number: 975-062

Location: Pichi Richi South Canyon

Mineralogy:

Quartz 40%
Calcite 40%
Albite 5%
Muscovite 5%
Chlorite 8-10%
Other 2%

Description: Laminated quartz and calcite rich and mica rich layers. Very fine grain (10 -50um) angular detrital quartzwith overgrowths. Equant ferroan calcite cement recrystallized microsparite.

Classification: Fine grain silty limestone (Calcisiltite or microsparite)

Sample Number: 975-067

Location: Pichi Richi South Canyon

Mineralogy:

Quartz 40%
Calcite 40%
Albite 5%
Muscovite 5%
Chlorite 8-10%
Other 2%

Description: Laminated quartz and calcite rich and mica rich layers. Very fine grain (10 -50um) angular detrital quartzwith overgrowths. Equant ferroan calcite cement recrystallized microsparite.

Classification: Fine grain silty limestone (Calcisiltite or microsparite)

Sample Number: 975-515

Location: Devils Peak Carbonate Platform

Mineralogy:

Quartz 20%
Calcite 20%
Dolomite 40%
Albite 5%
Muscovite 5%
Chlorite 8-10%
Other 2%

Description: Fine grained mixed dolomite and calcite. Sawtoothed twinned Albite and minor quartz. Highly recrystallized with prominant twinned dolomite.

Classification: Mixed dolomite -calcite

Sample Number: 975-075

Location: Devils Peak

Mineralogy:

Quartz 10%
Calcite 70%
Dolomite 5%
Albite 5%
Muscovite 3%
Chlorite 2%
Other opaques 2%

Description: Very fine grain (10 -50um) angular detrital quartz and minor albite with overgrowths. Equant ferroan calcite cement recrystallized to microsparite.

Classification: Fine grain silty limestone (Calcisiltite or microsparite)

Sample Number: 975-080

Location: Devils Peak Platform

Mineralogy:

Quartz 10%
Calcite 80%
Dolomite5%
Albite 5%
Muscovite 5%
Chlorite 3%
Other 10%

Description: Highly recrystallized limestone with very fine grain (10 -50um) angular detrital quartz. Calcite recrystallized to equant ferroan calcite burial cement and corse grained spar with abundant twining.

Classification: Micrite recrystalized to microsparite (Calcisiltite or microsparite)

Sample Number: 975-086

Location: Devils Peak Platform

Mineralogy:

Quartz 10%
Calcite 75%
Albite 2%
Muscovite3 %
Chlorite 3%
Other 7%

Description: Micritic intraformational conglomerate allochems with coarse grain sparite cement and micritic matrix Abundant stylonodular bedding and styolites. Late stage cross cutting secondary veins

Classification: Micritic intraformational conglomerate

Sample Number: 975-089

Location: Devils Peak Platform

Mineralogy:

Quartz 15%
Calcite 70%
Dolomite 5%
Albite 2%
Muscovite 3%
Other Opaques 2%

Description: Very fine grain (10 -30μm) angular detrital quartz with overgrowths. Micritic ferroan calcite recrystallized microsparite.

Classification: Recrystallized micritic limestone (microsparite)

Sample Number: 975-098

Location: Devils Peak Platform

Mineralogy:

Quartz 15%
Calcite 65%
Dolomite 8%
Albite 7%
Muscovite 4%
Chlorite 3%
Other 3%

Description: Micritic silty limestone with fine grain quartz and clay rich layer. Quartz and albite angular with irregular shape. Calcite micritic and recrystallization to microsparite.

Classification: Microsparite

Sample Number: 975-104

Location: Devils Peak Platform

Mineralogy:

Quartz 25%
Calcite 60%
Albite 5%
Muscovite 5%
Chlorite 3%
Other 2%

Description: Fine grain quartz (20-40μm) angular

Classification: Fine grain silty limestone (Calcisiltite or microsparite)

Sample Number: 975-111

Location: Devils Peak Platform

Mineralogy:

Quartz 45%
Calcite 40%
Albite 5%
Muscovite 3%
Chlorite 5%
Other 2%

Description: Fine grain quartz sandstone with equant mosaic ferroan microspar cement.

Classification: Fine grain Calcarous sandstone

Sample Number: 975-221

Location: Richman Valley Canyon

Mineralogy:

Quartz 30%
Calcite 50%
Albite 5%
Muscovite 5%
Chlorite 5%
Other 5%

Description: Silty limestone with aggergates of fine grained black opaques. Ferroan calcite cement and micite.

Classification: Fine grain silty limestone (Calcisiltite or microsparite)

Sample Number: 975-301

Location: Richman Valley Canyon

Mineralogy:

Quartz 35%
Calcite 45%
Albite 5%
Muscovite 5%
Chlorite 2%
Other 3%

Description: Laminated quartz and calcite, and mica rich layers. Very fine grain (10 -50um) angular detrital quartz with overgrowths. Equant ferroan calcite with minor non ferroan calcite cement. Recrystallized to microsparite and sparry calcite.

Classification: Fine grain calcarous silty sandstone

Sample Number: 975-317

Location: Waukarie Creek Canyon

Mineralogy:

Quartz 20%
Calcite 60%
Dolomite 5%
Albite 4%
Muscovite 5%
Chlorite 3%
Other 3%

Description: Very fine grain (10 -50um) angular detrital quartz with overgrowths. Equant ferroan calcite cement and micrite Recrystallized microsparite.

Classification: Fine grain silty limestone (Calcisiltite or microsparite)

Sample Number: 975-322 (Wallplaster)

Location: Waukarie Creek Canyon

Mineralogy:

Quartz 10%
Calcite 75%
Dolomite 5%
Albite 5%
Muscovite 2%
Chlorite 1%
Other 2%

Description: Highly Calcareous, very fine grained ferroan micrite Manganese dendrites and cross cutting sparry calcite veins. Euhedral albite probably authogeneic and embayed alkaline attacked quartz.

Classification: Micritic limestone

Sample Number: 975-324

Location: Waukarie Creek Canyon

Mineralogy:

Quartz 20%
Calcite 65%
Albite 6%
Muscovite 7%
Chlorite 2%
Other 3%

Description: Very fine grain (10 -50um) angular detrital quartz with overgrowths and embayments. Equant ferroan calcite cement and micrite.

Classification: Fine grain silty limestone (Calcisiltite or microsparite)

Sample Number: 975-404

Location: Richman Valley Canyon Cut.

Mineralogy:

Quartz 10%
Calcite 75%
Dolomite 5%
Muscovite 4%
Chlorite 3%
Other 3%

Description: Micritic clast supported intraformational conglomerate.

Classification: Micritic limestone (Calcisiltite or microsparite)

Sample Number: 975-407B

Location: Richman Valley

Mineralogy:

Quartz 10%
Calcite 75%
Dolomite 5%
Muscovite 5%
Chlorite 3%
Other 2%

Description: Micritic intraformational conglomerate. Clast supported

Classification: Fine grain silty sandstone (Calcisiltite or microsparite)

Appendix 4 Sections

Ilchi Richi South Canyon
Devils Peak Carbonate Platform
Richmond Valley Canyon
Waukarie Creek Canyon

Devils Peak - Carbonate Platform

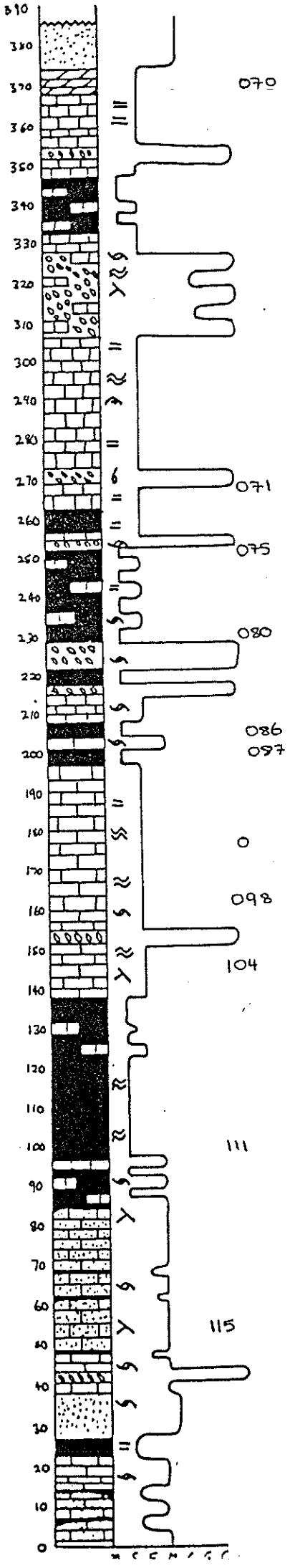

Legend

- Parallel Lamination
- Wavey Bedding
- Truncated Bedding
- Hummocky Cross Stratification
- Planar Cross Bedding
- Trough Cross Bedding
- Stylonodular Bedding
- Ripple Marks
- Flute Casts
- Load Casts
- Slump
- Stylolite
- Mud Flakes

Lithology

- Limestone
- Sandy Limestone
- Calcareous Sandstone
- Shale
- Intraformational Conglomearate
- Dolomite

Pichi Richi South - Canyon

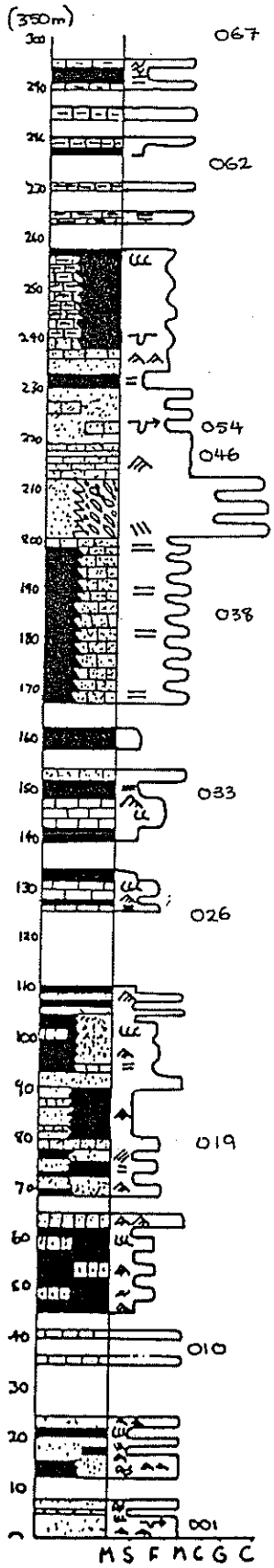

Legend

- Parallel Lamination
- Wavey Bedding
- Truncated Bedding
- Hummocky Cross Stratification
- Planar Cross Bedding
- Trough Cross Bedding
- Stylonodular Bedding
- Ripple Marks
- Flute Casts
- Load Casts
- Slump
- Stylolite
- Mud Flakes

Lithology

- Limestone
- Sandy Limestone
- Calcareous Sandstone
- Shale
- Intraformational Conglomearate
- Dolomite

Richmond Valley - Canyon

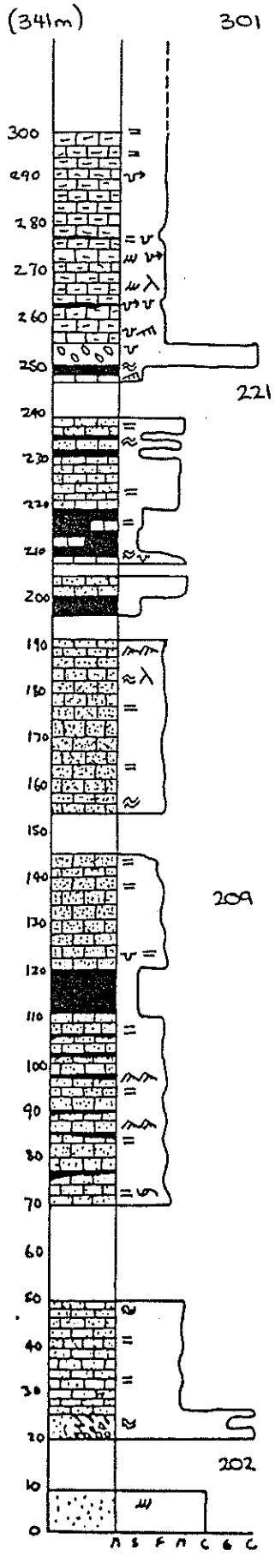

Legend

=	Parallel Lamination
≈	Wavey Bedding
⋋	Truncated Bedding
⌇	Hummocky Cross Stratification
//	Planar Cross Bedding
CCC	Trough Cross Bedding
∞	Stylonodular Bedding
⩘	Ripple Marks
⌇→	Flute Casts
⌇	Load Casts
6	Slump
⌇	Stylolite
⌇	Mud Flakes

Lithology

- Limestone
- Sandy Limestone
- Calcareous Sandstone
- Shale
- Intraformational Conglomearate
- Dolomite

Waukarie Creek Canyon-Sample Locations

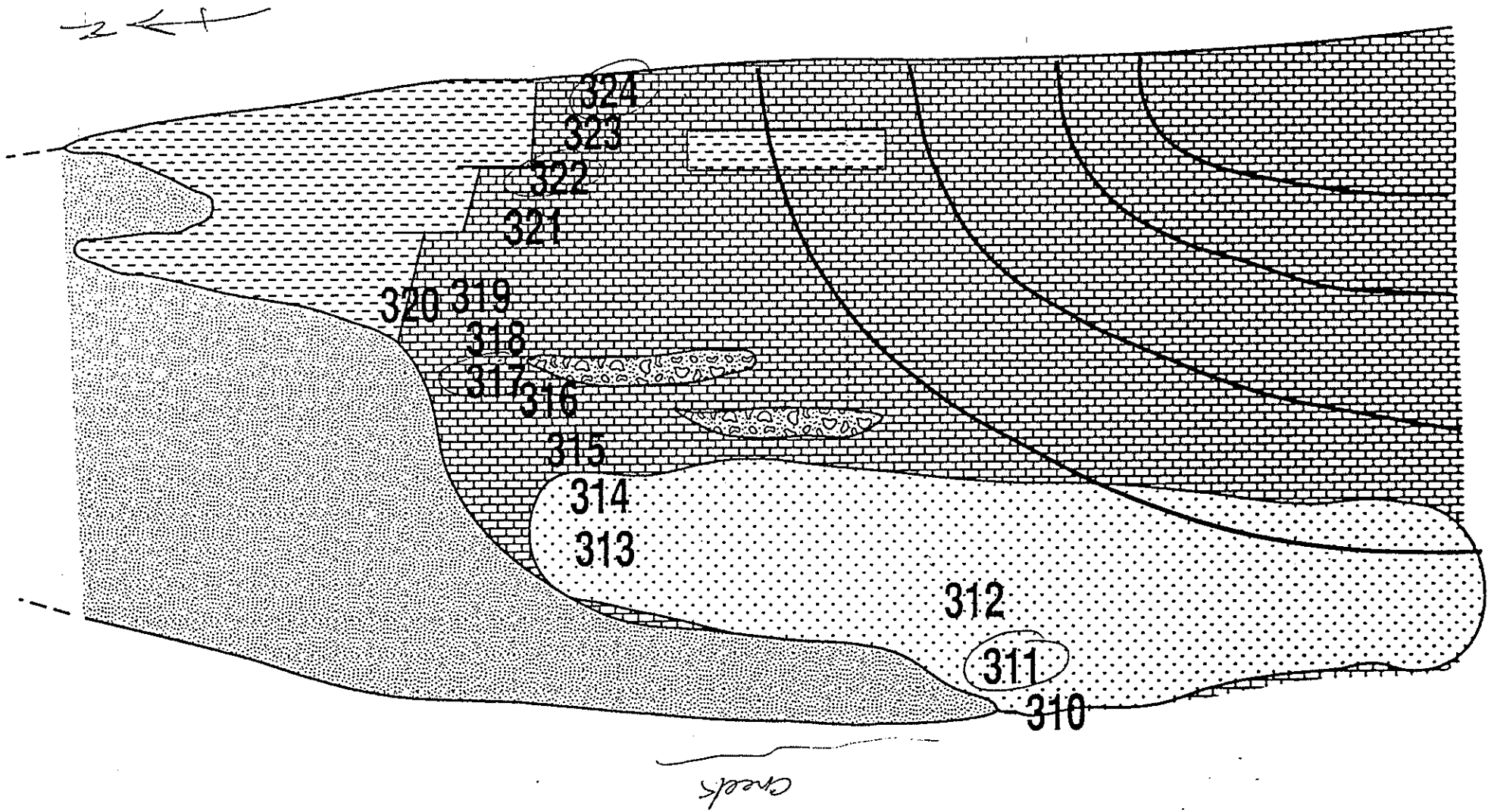

GEOLOGY OF WONOKA FORMATION PICHI RICHI PASS SOUTHERN FLINDERS RANGES SOUTH AUSTRALIA

Legend

Geological Boundary
- Established
- Inferred

Fault
- Established
- Inferred

Bedding
- Trend
- Dip / Strike
- Vertical
- Horizontal
- Overturned
- Syncline
- Anticline

- Road
- Track
- Railway Line
- Creek
- Homestead

Magnetic North / North

Stratigraphy

Hawker Group
- Rawnsley Quartzite
- Bunyeroo Formation

Wilpena Group

Wonoka Formation — Carbonate Platform
- Unit 8
- Unit 7
- Unit 6
- Unit 5
- Transitional Unit

Wonoka Formation — Canyon
- Multicoloured Unit
- Green Limestones and Shales
- Basal Sands
- Intraformational Conglomerate
- Olistrostrome Unit
- Wallplaster

- Bunyeroo Formation
- ABC Range Quartzite
- Brachina Formation
- Nuccalenna Formation

Umberatana Group

Locality Map